

LIBRARY
ROYAL AIRCRAFT ESTABLISHMENT
BEDFORD.



MINISTRY OF AVIATION
AERONAUTICAL RESEARCH COUNCIL
CURRENT PAPERS

The Effect of External Flow
on an Internal-expansion Propelling Nozzle
Incorporating Ventilation by Ambient Air

By

M. V. Herbert, C. Overy, R. A. Pinker and G. T. Golesworthy

LONDON · HER MAJESTY'S STATIONERY OFFICE

1966

Price 10s. 0d net

The effect of external flow on an internal-expansion propelling
nozzle incorporating ventilation by ambient air

- by -

M. V. Herbert, C. Overy, R. A. Pinker and G. T. Golesworthy

SUMMARY

Previous attempts to improve the off-design performance of a convergent-divergent nozzle evolved the principle of "ventilation". This provides for the transmission of ambient pressure to the over-expanded divergent surfaces, by means of small quantities of secondary air induced from atmosphere. The technique has been developed to operate satisfactorily at low pressure ratio in quiescent air, using successive stages of secondary air admission. A penalty is paid, however, in that design-point performance is somewhat reduced.

In external flow, low nozzle base pressures are created, supplanting ambient pressure as the environment into which the nozzle exhausts. With a fairly high subsonic or transonic external stream, ventilation has been found incapable of raising the level of base pressure. Under these conditions, the technique offers no useful improvement in nozzle internal performance at low pressure ratio.

CONTENTS

	<u>Page</u>
1.0 Introduction	4
2.0 Previous work	4
3.0 Test equipment	7
3.1 Pressure plotting rig	7
3.1.1 Air supplies	7
3.1.2 Thrust measurement	7
3.2 Thrust rig	8
3.3 Model geometry	9
4.0 Quiescent air tests	10
4.1 Single-stage builds	10
4.2 Two-stage builds	12
5.0 External flow tests	14
6.0 Conclusion	15
Acknowledgement	15
References	16

Detachable abstract cards

APPENDICES

<u>No.</u>	<u>Title</u>	
I	Notation	17
II	Definitions	18

ILLUSTRATIONS

<u>Fig. No.</u>	<u>Title</u>
1	Ventilation slot geometry
2	Arrangement of model
3 and 4	Single-stage nozzle efficiency in quiescent air
5 to 8	Single-stage nozzle pressure distribution
9 and 10	Secondary mass flow
11 to 13	Two-stage nozzle efficiency in quiescent air
14	Running-full lines
15 to 17	Two-stage nozzle efficiency in external flow
18 and 19	Ventilation slot pressures
20 to 24	Two-stage nozzle pressure distribution
25	Pressure distribution in various nozzles

1.0 Introduction

For flight at medium supersonic speeds, a propelling nozzle is required having a design pressure ratio in the range 15 to 30. If an arrangement with wholly-internal expansion is used, the performance when operated at low pressure ratio is very poor - a situation which results from much of the divergent nozzle surface experiencing pressures below ambient. The loss at such conditions can present a serious problem, since take-off thrust is important, as may also be the capability for economical aircraft operation at subsonic speed.

In order to improve this off-design performance, it is necessary to increase the sub-ambient pressures acting within the nozzle. Boundary layer separation already affords a natural means whereby extreme depression is prevented, and, for a given boundary layer state, what is desired is to induce permanent separation more readily by some artificial device; that is, to encourage detachment of the main jet from the nozzle walls further upstream. By permanent separation is meant separation with no subsequent reattachment. Boundary layer separation in supersonic flow can be produced quite easily - for example, by a rearward-facing step or abrupt change of curvature - but that is not enough. Unless the pressure downstream of separation can be maintained at a level close to that of the nozzle environment, reattachment will quickly occur and the jet will continue to over-expand.

The essential need in these circumstances is to transmit substantially ambient pressure into a region of artificially promoted separation. To be successful, this transmission process must obviously not itself involve any serious losses, and only small quantities of secondary air at a low energy level can be countenanced. This principle has been termed "ventilation".

2.0 Previous work

Some early tests by Crosse¹ in quiescent air, using nozzles with conical divergence and design pressure ratio up to 10, demonstrated that a ventilation slot in the form of a hollow circumferential step in the nozzle wall is capable of improving performance at low pressure ratio, the plenum chamber behind the slot being open to atmosphere. Although the induced secondary air could be shut off externally at conditions near the design-point, the discontinuity in wall profile formed by the step remained. Since the whole purpose of the exercise was to achieve an "aerodynamically variable" nozzle, mechanical means to eliminate the step were not considered, and it must represent some loss in design-point performance.

The slot geometry finally employed in Reference 1 was similar to Figure 1(a) with a step angle of 20° , and Crosse investigated variation of vent area ratio $\frac{A_1}{A_2}$ from 1.0 (step at the throat) to 1.21 (vent pressure ratio 4). Secondary mass flow quantities were measured, and found to decrease from around 7 per cent of primary flow at pressure ratio 2 to near zero with increase of pressure ratio. It was thought that some outward leakage of primary air would eventually occur unless the plenum chamber entry was closed.

More comprehensive tests² were later carried out in continuation of this work, using the same scale of model (2 in. diameter throat) and still

exhausting into quiescent air. In the majority of cases, models were supplied with cold wet air as in Reference 1, but cold dry air was used in some of the later tests to obtain design-point performance. Among the features studied were:-

- (i) Step angle: standard values were 10° , 15° and 20° , achieved by variation of step length, keeping constant step height.
- (ii) Step area ratio $\frac{A_2}{A_1}$: standard values were 1.17 and 1.09, varying step length and height together.
- (iii) Direction of injection, as in Figures 1(a), (b) and (c).
- (iv) Vent pressure ratio, using values 3.1, 3.7, 4 and 5 corresponding one-dimensionally to $\frac{A_1}{A_g}$.
- (v) Nozzle design pressure ratio, using values 8.2, 10, 15 and 20.
- (vi) Successive staging of ventilation in the nozzles of higher design pressure ratio.

All models in the programme above were axisymmetric with conical divergence of 10° half-angle.

In the case of step angle, a compromise was sought between design-point loss and the effectiveness in promoting separation at low pressure ratio. Not all test results were unanimous on this point, but it can generally be said that step angle had comparatively little influence over the range tested. In no circumstances were values in excess of 15° found to offer advantage.

Step area ratio $\left(\frac{A_2}{A_1}\right)$ had a more marked effect; the lower value tested produced appreciably worse off-design performance. This was presumed to be associated with a reduction in secondary flow.

With regard to the direction of injection, this would not be expected to affect design-point operation at all, since no secondary air was then admitted. In fact, performance at low pressure ratio was also found to be insensitive to it, implying that the amount of momentum in the secondary air leaving the ventilation slot was so small a proportion of that in the mainstream that it could be thrown away without detectable loss. But if it should be required to discharge air from a high pressure source in the same manner, then the nearly-axial slot could be preferable, as offering more chance for the potential thrust of the secondary air to be realised. Secondary flow quantities were measured, and shown to be effectively independent of the direction of injection.

Perhaps the most important aspect of the tests was that concerned with the effects of vent pressure ratio and nozzle design pressure ratio (D.P.R.), and the use of multi-staging. These are to some extent inter-related. In a nozzle of D.P.R. 10 and below, a single ventilation stage was found to be adequate; and location of the peak performance at low operating pressure ratio, or "first peak", could be adjusted to some extent by variation of vent pressure ratio (V.P.R.). For example, change of

V.P.R. from 3.1 to 5.0 produced a shift of this first peak from pressure ratio 2.6 to 3.8.

With D.P.R. above 10, the choice as to number of stages would depend on the design requirements. To maintain improved performance in a nozzle of D.P.R. 20 throughout the range of operating pressure ratio, it was found that two stages of ventilation were necessary, but this of course could entail an increased cost in terms of design-point loss. A single stage was still able to give high gains over a narrow band of pressure ratio.

A limited amount of work was also done with an axisymmetric internal-expansion nozzle of D.P.R. 10, having $7\frac{1}{2}^\circ$ half-angle outer walls and a 15° half-angle conical centrebody which, by translation, would be capable of providing variation of throat area in the ratio 4:3. Ventilation was applied only to the outer walls, but the test results indicated that the general pattern of behaviour was little affected by the presence of the centrebody, and that there was no case for its surface to be ventilated also.

In addition, some further tests were carried out on square-section models of D.P.R. 10, with all four walls diverging at 10° half-angle. A very marked improvement in off-design performance was realised by ventilation of two opposite walls, but the further gain from ventilation of all four was fairly small, while the secondary mass flow doubled. Provision of steps on all four walls and air admission to opposite walls only was not found to be a useful arrangement.

No alternative designs of ventilation slot were tested in either the centrebody or square nozzles.

From all the foregoing work, it could be concluded that, in quiescent air, the technique of ventilation offers a general means for obtaining considerable improvement in off-design performance of any internal-expansion nozzle, at the cost of some design-point loss. Ultimate success or failure then depends on the effect of external flow.

In the presence of an external stream, a low nozzle base pressure is created, supplanting ambient pressure as the environment into which the nozzle exhausts. The performance of an internal-expansion nozzle at low exhaust pressure ratio $\left(\text{E.P.R.} = \frac{P_t}{P_\infty} \right)$ is naturally worse under these conditions, as a result of further internal over-expansion. To improve the situation the base pressure must be raised. Strong hope existed that admission of secondary air at nearly ambient pressure within the nozzle would produce a region of separated mainstream flow in which the pressure was at least considerably higher than the original base pressure. Thus the crucial question remaining was whether ventilation in external flow can continue, reiterating the words of Section 1.0, "to transmit substantially ambient pressure into a region of artificially promoted separation". The further tests described in the following sections were arranged to provide the answer.

3.0 Test equipment

3.1 Pressure plotting rig

A description of the composite rig used for the majority of these tests appears in Reference 3. Models could be mounted in three alternative ways, two of which provided external flow in different speed bands, and the other was for quiescent air tests. In all three arrangements there was a common supply system to the model, which was carried on a long parallel hollow sting of $3\frac{1}{2}$ in. overall diameter. This consisted of two co-axial tubes, the inner supplying air to the model, while instrumentation lines passed through the annular gap between them.

For external flow in the range of Mach number 1.3 to 2.5, a two-dimensional flexible wall nozzle of 12 in. x 12 in. outlet was used. A slotted nozzle of circular cross-section, 11.3 in. diameter, enabled external Mach numbers to be produced between 0.7 and 1.5. The sting assembly mentioned above was arranged to pass centrally through the throat of either external flow nozzle. Quiescent air tests could be carried out either by enclosing the end of the sting in a depression chamber, connected to a diffuser system for pressure recovery, or by discharging the model air directly to atmosphere. In the present work the latter arrangement was employed.

3.1.1 Air supplies

Both model and external flow lines were fed with dry air at stagnation temperatures around 35°C . Air dryness was measured by an R.A.E.-Bedford pattern frost-point hygrometer, and held at better than -20°C .

Air supply pressure was at an initial level of approximately 5 atm, throttled independently as required for the various lines. Model throat Reynolds number in this rig for the tests here reported lay in the band 1.1 to 3.7 million, which would imply[†] a turbulent boundary layer throughout.

3.1.2 Thrust measurement

Means for direct measurement of model thrust were not available in this rig, and it was necessary to rely on pressure plotting. Gross thrust of the model was then determined by summation of the stream thrust in the throat plane (obtained by calculation) and the thrust upon the divergent surfaces (given by the pressure tappings). The expression for gross thrust efficiency[†] is then as derived in Reference 6:-

$$\eta_F = \frac{1.26789 C_D \cdot \mu + \int_1^{A_e/A_g} \frac{P_w}{P_t} d\left(\frac{A}{A_g}\right) - \frac{1}{\text{E.P.R.}} \left(\frac{A_e}{A_g}\right) - \phi}{0.0123156 C_D \left[\frac{v}{\sqrt{T_t}} \right]_{\text{EPR}}}$$

[†] For definition see Appendix II

taking $\gamma = 1.4$. This depends upon knowledge of the following quantities:-

- (i) Discharge coefficient (C_D). This was derived from tests on a quiescent air rig equipped for mass flow measurement. When choked, a value of 0.991 was found to be appropriate to the models in these tests.
- (ii) Throat vacuum thrust efficiency (μ), taken to be 1.003 when choked, as obtained in Reference 4 for similar throat geometry (see Section 3.3).
- (iii) Exhaust pressure ratio $\left(\text{E.P.R.} = \frac{P_t}{P_\infty} \right)$, obtained from a pitot rake at model entry and static pressure measured either at the wall of the working section in external flow tests, or in the model surroundings for quiescent air tests.
- (iv) Computed allowance for internal friction downstream of the model throat (ϕ). This can be obtained from curves presented in Reference 4, by adding together what are there termed the "momentum loss" and "displacement loss". In these tests, the quantity amounts to a deduction of approximately 0.7 per cent from gross thrust efficiency.

It should be noted that, in the above relation for η_T , no account is taken of the drag force acting on the thin annular base of the model. Furthermore, no allowance is made for any drag associated with the use of secondary air. If secondary air is supplied at a pressure above P_∞ , then, in addition to any change in the numerator, the denominator should include a further term appropriate to the potential thrust of that air when expanded isentropically and separately; this, however, does not arise in the present tests.

While there is no fundamental limitation to accuracy in this method of obtaining thrust efficiency from pressure plotting, experience has suggested that in practice the results cannot be guaranteed better than $\frac{1}{2}$ per cent, generally above the true value. This is adequate for investigation of off-design performance, as in a lot of external flow work where one is mainly concerned with low efficiencies, but certainly not good enough at the design-point. Fortunately, as has been demonstrated in Reference 3 and elsewhere, the design-point efficiency of an internal-expansion nozzle is independent of external flow conditions, as indeed is the whole running-full line. For such a nozzle, the only effect of external flow is to change the value of E.P.R. at which performance departs from the running-full line. Hence the design-point tests could in this case more satisfactorily be carried out on a quiescent air rig where direct thrust measurement was available.

3.2 Thrust rig

For some quiescent air tests at higher E.P.R., and especially those in the vicinity of the nozzle design-point, use was made of another rig, described in Reference 4. This was capable of measuring both mass flow and thrust directly. Supply air was dry (better than -20°C frost-point) and cold (around 10°C), but restricted to 1 atm pressure, giving a model throat Reynolds number of only 0.75 million. Control of operating pressure ratio was achieved by varying the suction from an exhaust manifold, into which the test model discharged via a pressure recovery system.

At the above value of Reynolds number, the boundary layer at the nozzle throat is known to be laminar^{4,5}. It has been found, however, that a major discontinuity in the divergent wall, such as a ventilation slot, will bring about boundary layer transition. Thus in the present tests, any flow separation occurring downstream of the first slot would be naturally turbulent in character.

In order to ensure a turbulent boundary layer throughout for consistency with the other tests (Section 3.1.1), recourse was had to a technique based on the work of Cook⁷, and successfully adopted before on the same rig⁴. The method consists of spreading silicon carbide powder of No. 150 grade thinly on a paint base, to form a band around the model periphery in the convergent section. For this scale of model with 2 in. diameter throat, the band was $\frac{1}{8}$ in. wide, and its downstream edge $\frac{1}{2}$ in. ahead of the plane of minimum area.

3.3 Model geometry

Two basic forms of axisymmetric model embodying different arrangements of ventilation slot were designed for the external flow tests, and one of these is illustrated in Figure 2. In that case the ventilation slots correspond to "undirected" injection as shown in Figure 1. The second model had "axial" injection. Some parts were common to both models, but the throat and divergent sections were different in each. For both, first and second-stage vent pressure ratios were 3.7 and 10 respectively, the overall design pressure ratio 20 (plane area ratio throat to outlet 2.90), and wall semi-angles 10° . Throat diameters were 2.00 in., and the blend between approach and divergent portions of wall profile consisted of 1.0 in. circular arcs. This throat geometry was identical to that of the plain conical nozzle of same D.P.R. tested in Reference 3. Other common features were the parallel afterbody and narrow annular base 0.050 in. wide at outlet.

Details of ventilation slot geometry were as given below:-

	Undirected injection	Axial injection
Step angle (nominal)	20°	16°
Step length	0.154	0.188
Step height	0.088	0.094
Lip thickness	0.050	0.013
$\frac{A_2}{A_1}$ { first vent	1.17	1.18
{ second vent	1.13	1.14
$\frac{A_1}{A_g}$ { first vent	1.18	1.18
{ second vent	1.93	1.93

Wall pressure tappings were fitted in each model as follows, with hole diameters 0.020 in.:-

- (i) Ten in all, spirally positioned down the three portions of conical divergent profile.
- (ii) One facing downstream in each of the two ventilation slot lips (see Figure 1).
- (iii) One in each of the two secondary flow plenum chambers.
- (iv) One in the base annulus.
- (v) Two on the external surface of the afterbody, one ahead of each row of secondary air inlet ports.

Although in principle secondary air could be supplied from any convenient source, it has become customary, following Crosse¹, for it to be drawn directly from atmosphere. This arrangement was again adopted in the present models. Each ventilation slot was fed from a separate annular plenum chamber within the thickness of the model (Figure 2), which in turn communicated with the surrounding atmosphere through a circumferential row of circular ports cut in the cover sleeve. For tests with either vent closed, the appropriate cover sleeve was replaced by one without ports.

As can be seen from Figure 2, each basic design of model was made up of a number of pieces forming successive sections of nozzle surface. In quiescent air, where afterbody shape and base thickness are not important, the final section of each model could be omitted, to leave nozzles of D.P.R. 10 having one stage of ventilation at pressure ratio 3.7, either with undirected or axial injection. Thus for each model there were five builds of interest:-

- (a) Single stage, D.P.R. 10: vent open
- (b) vent closed
- (c) Two stages, D.P.R. 20: both vents open
- (d) first vent closed, second vent open
- (e) both vents closed

4.0 Quiescent air tests

We shall refer to that part of a nozzle between throat and upstream end of the first ventilation slot as the "first section", and use "second section" to denote the part from downstream end of the first slot to outlet (in the case of a single-stage build) or upstream end of the second slot (in the case of a two-stage build). When dealing with two-stage nozzles, "third section" will relate to the wall between downstream end of the second slot and outlet.

4.1 Single-stage builds

With vent open, Figures 5 and 7 show the wall surface pressures within the nozzle for undirected and axial injection respectively, over a

range of E.P.R. The effective pressure acting on the projected area of the ventilation slot has been drawn as uniform and equal to the downstream-facing lip pressure for lack of any better information.

Taking first the results for undirected injection, it can be seen that both P_1 and P_b approximate closely to P_∞ . At E.P.R. up to $2\frac{1}{2}$, separation is occurring within the first section; at higher E.P.R., either a shock or expansion originates at the vent lip (station 1 in Figure 1), in order to bring about the necessary change of pressure to P_1 . The second section is running fully separated and quite close to ambient pressure up to E.P.R. $3\frac{1}{2}$. At E.P.R. 4 the flow has partly attached to the second section, with separation taking place fairly near the outlet. Above E.P.R. 5 the nozzle is running full. Axial injection gives a substantially similar picture, with vent pressures generally rather lower.

In terms of gross thrust efficiency, the results appear in Figures 3 and 4. The "first peak", already referred to in Section 2.0, occurs at E.P.R. near 3; and the subsequent fall in efficiency, to a minimum at E.P.R. around 4, corresponds to progressive attachment to the second section. At higher E.P.R. the curves rise again steadily in a manner similar to any other nozzle running full, to peak near the value of D.P.R.

Figures 6 and 8 give wall pressures with vent closed. For both nozzles P_1 is always further below P_∞ than was the case with vent open, even when the second section is fully separated. With increasing pressure ratio, the second section remains separated up to a value of E.P.R. very close to 3, where an abrupt change of flow regime takes place. The separation shock then moves suddenly to a position near the nozzle outlet, with the flow up to that point becoming attached to the second section, and bridging the ventilation slot by a sequence of expansion and shock. In this respect the nozzles with undirected and axial injection show identical behaviour. However, the expansion at the vent lip after attachment corresponds to a supersonic turning angle which is different for the two nozzles, being 18.3° with undirected injection and 15.8° in the axial case. These figures may be compared with the values of nominal geometric step angle of 20° and 16° mentioned in Section 3.3, suggesting that the flow reattaches at or very shortly downstream of the beginning of the second section in both nozzles. It is probable that the direction of injection has no special influence at these conditions.

With further increase of E.P.R. the nozzles eventually run full; this occurs around E.P.R. 5, the same as with vent open. Once the nozzles are running full, the outlet pressure in both is about $\frac{P_t}{8}$, as compared with the isentropic figure of $\frac{P_t}{10}$ appropriate to the area ratio.

Some hysteresis accompanies the sudden change of flow pattern, and with decreasing pressure ratio the critical value of E.P.R. for shock movement is slightly below 2.5. Figures 6 and 8 include pressure distributions just before and just after shock movement, approaching from either direction.

These effects are clearly reflected in the efficiency curves of Figures 3 and 4. So long as the second section remains completely separated, there is no very great difference between the values of thrust efficiency with vent open or closed, and what difference there is would be partly counteracted by drag associated with collecting the secondary air.

As the shock pattern changes with vent closed, the sudden shift of efficiency amounts to nearly 10 per cent; the performance thereafter is no better than that of a nozzle of the same area ratio without a ventilation slot. In the range of E.P.R. $2\frac{1}{2}$ to 4, therefore, secondary air is clearly beneficial.

From then on the efficiency curves for vent open and closed gradually approach one another, and the choice of E.P.R. at which to close the vent would depend upon knowledge of secondary flow quantities, and the drag penalty associated with its use throughout a flight path. Where secondary flow is taken on board from flush ports in the afterbody, as in the present models, some calculations have suggested that 1 per cent of flow would cost on average about $\frac{1}{2}$ per cent of gross thrust in flight, at typical conditions within the range of interest. Figure 9 gives mass flow ratio as a function of E.P.R. for an undirected injection model of identical slot geometry (in quiescent air), and previous work has indicated that the direction of injection makes little difference (Section 2.0). However, in the present tests, the effective discharge area of the ventilation slot was, with axial injection, only about 70 per cent of that with undirected; thus some reduction in secondary flow may be expected in the axial case. As a guide for general purposes, we can take it that the vent might remain open up to E.P.R. around 7.

4.2 Two-stage builds

Wall pressure distributions with both vents open will be found in Figures 20a and 22 for undirected and axial injection respectively. It can be seen that, so far as the first and second sections are concerned, the patterns are generally similar to those in Figures 5 and 7 obtained without the third section present. This third section is completely separated at all values of E.P.R. up to 6. Curves of thrust efficiency within this range should therefore resemble those for single-stage nozzles with vent open (Figures 3 and 4), and in fact do so appear in Figures 11 and 12. Actual levels in the latter are somewhat lower, however, since the extra surface of the two-stage nozzles is at slightly sub-atmospheric pressure.

When the first vent is closed and the second open, wall pressures become as shown in Figures 21a and 23, for E.P.R. increasing only. Once again, the first and second sections behave very much the same as without the third (see Figures 6 and 8). The third section is fully separated up to E.P.R. 6, as it was with both vents open; consequently the appropriate efficiency curves in Figures 11 and 12 below that condition are similar in shape to those for single-stage nozzles with vent closed (Figures 3 and 4), but somewhat lower in level.

At higher E.P.R. with first vent either open or closed and second vent open, the flow becomes attached to the third section, which eventually runs full above E.P.R. 12. This process of reattachment downstream of an open vent is a gradual one, as was seen with single-stage nozzles, and does not involve sudden travel of the separation shock. Nor is any hysteresis found with E.P.R. increasing and decreasing. Attachment to the third section is accompanied by a further sequence of peak and trough in the efficiency curves (Figures 11 and 12), and this feature has been called "second peak". In general one can say that there will be as many subsidiary peaks below the design-point as there are stages of ventilation.

For operation in the neighbourhood of the design-point, both vents would be closed, and at that condition attention need normally be directed only to the case of nozzle running full (E.P.R. > 12 with these models). If tested, however, the complete range of performance should include two successive occurrences of sudden shock travel as the flow reattaches downstream of closed vents. On Figure 14 are shown running-full pressure distributions for both undirected and axial injection models, and for a plain conical nozzle of the same D.P.R. and wall angle (from Reference 3). From these have been derived the following values of supersonic expansion angle at the various vents:-

	Undirected injection	Axial injection
First vent turning angle	18.5°	16.1°
Second vent turning angle	15.8°	15.6°
Step angle for both vents (nominal)	20°	16°

It seems that the turning angle in the first vent follows fairly closely the geometric value in this range, while in the second vent the turning angle is limited to something like 16° regardless of geometry.

Efficiency curves for all three vent arrangements with undirected injection are plotted together in Figure 13. Secondary mass flow quantities are given in Figure 10, again for an undirected injection model of identical slot geometry (in quiescent air). On the same basis of calculation as in Section 4.1, these results would suggest that the first vent might be closed between E.P.R. 6 and 7, and the second vent around E.P.R. 13.

Also shown in Figure 13 for comparison is the performance of the plain conical nozzle of Reference 3. Those data were obtained entirely from pressure plotting, and the authors of that paper recommend that the value of design-point efficiency given should be regarded as about 0.3 per cent too high; accordingly the level in Figure 13 has been adjusted by this amount (to 0.988). It is interesting to note that, when tested in quiescent air on a different thrust rig⁸, a geometrically similar conical nozzle with 6 in. diameter throat and D.P.R. 21 produced a mean value of design-point efficiency of 0.9885. In the latter case the nozzle was supplied with air at approximately the same temperature and pressure as that of Reference 3, so that a factor of 3 existed on throat Reynolds number; this should represent a difference of about 0.07 per cent in design-point efficiency between the nozzles of References 3 and 8, implying a level of 0.9878 for the conical nozzle in Figure 13.

Ascough⁸ also tested at design-point a two-stage ventilated nozzle built up from the same 6 in. diameter throat section, with axial injection and 15° step angles, being thus similar to one of the smaller models used

in the present tests. He obtained a mean efficiency value of 0.981, thus implying that two ventilation slots incur a design-point loss of 0.75 per cent. As the following table shows, a rather higher figure for this loss is suggested by the smaller scale test results.

Design-point thrust efficiencies

	6 in. scale (Reference 8)	2 in. scale
Plain conical nozzle D.P.R. 20	0.9885	0.988 (estimated)
Two-stage ventilated nozzle Undirected injection D.P.R. 20	-	0.976
Two-stage ventilated nozzle Axial injection D.P.R. 20	0.981	0.976

In any flight scheme, there will be some exchange rate between the worth of design-point and off-design performance. Hence, before any overall benefit is derived from the use of ventilation, there must be a gain at low E.P.R. which is sufficient to offset the design-point loss factored by this exchange rate.

5.0 External flow tests

Values of thrust efficiency for the two-stage nozzle with undirected injection and both vents open are presented in Figure 15 for the range of external Mach number 0.7 to 1.5. Also included are the quiescent air data taken from Figure 11. Further efficiency values appear in Figure 16 for the same nozzle with first vent closed and the second open, at Mach numbers from 1.5 to 2.0. Results for undirected and axial injection in subsonic external flow are shown together in Figure 17. On both Figures 15 and 16 are also given comparable curves for the plain conical nozzle of Reference 3, obtained from the same test rig and with the same boundary layer conditions. It is clearly apparent from these results that in external flow the performance with ventilation is effectively no better than that without. Sic transit spes.

Why? To answer this we must examine the internal pressures. Those most critical to the behaviour of a ventilated nozzle arrangement are, of course, the pressures in the vent slots themselves; these must evidently be close to ambient pressure for successful operation. The ratios of the two vent lip pressures to ambient are plotted in Figures 18 and 19, for undirected and axial injection respectively. It can be seen that, with increase of external Mach number, the first lip pressure (P_1) falls substantially below ambient at low E.P.R., while the second (P_2) is consistently lower still. These effects are even more pronounced with axial injection than with undirected.

A study of base pressures affords further and conclusive evidence of failure. Figures 18 and 19 show base pressures also, together with those for a plain conical nozzle at the same conditions. Marked similarity in pattern appears, and this comparison leads to the crucial conclusion that ventilation has brought about no general or worthwhile increase of base pressure. Moreover, it may be noted that at low E.P.R. P_2 is little removed from P_b ; so it becomes clear that the base pressure is not only unchanged, but is in fact still governing much of the region in which flow separation takes place. Similar low values of thrust efficiency for each type of nozzle are therefore inevitable.

Examples of complete pressure distributions are given in Figures 20b to 20e and 21b for undirected injection, over a range of E.P.R. at different external Mach numbers, and the levels of P_∞ and P_b are marked in each case. The curves of Figure 24 were derived by a process of interpolation, and show the effect of Mach number at constant E.P.R.

Finally, in Figure 25 the pressure distributions in three nozzles are compared at similar conditions of E.P.R. and M_∞ : the undirected and axial ventilated systems with both vents open, and the plain conical nozzle of Reference 3. Bearing in mind that the area under such a graph represents the divergent thrust, it may be observed, as would now be expected, that neither ventilated arrangement differs very greatly from the conical. Between themselves, the axial injection has lower pressures than the undirected in both first and second vent slots throughout, while sometimes producing higher pressures on the second and third section surfaces.

6.0 Conclusion

In an internal-expansion nozzle operating in quiescent air, ventilation can maintain separated flow at substantially ambient pressure over the greater part of the divergent surfaces which are otherwise subject to pressures below ambient, thereby reducing the loss in gross thrust efficiency from over-expansion at pressure ratios far below the design. On the debit side, there is a design-point loss introduced by the discontinuity in internal wall profile.

When such a nozzle is surrounded by external flow, a low base pressure is created which supplants ambient as the back-pressure to any system of flow separation within the nozzle, and thus causes greater over-expansion. Any large improvement in off-design performance can only be achieved by raising this base pressure. With a fairly high subsonic or transonic external stream, it has been found that ventilation is no longer capable of transmitting ambient pressure to the internal surfaces, and has scarcely any effect upon base pressure. Under these conditions, therefore, the technique offers no advantage.

ACKNOWLEDGEMENT

The authors wish to thank Miss M. Faiers and Miss V. Searle for their assistance in the test programme.

REFERENCES

<u>No.</u>	<u>Author(s)</u>	<u>Title, etc.</u>
1	G. W. Crosso	The development of an aerodynamically variable convergent-divergent propelling nozzle. A.R.C.21 915. February, 1960.
2	M. V. Herbert Flt. Lt. C. Sutcliffe R.A.F. C. Overy	Unpublished work in M.O.A. 1961.
3	G. T. Golesworthy M. V. Herbert	The performance of a conical convergent-divergent nozzle with area ratio 2.9 in external flow. A.R.C. C.P.891. November, 1963.
4	M. V. Herbert D. L. Martlew	The design-point performance of model internal-expansion propelling nozzles with area ratios up to 4. A.R.C. R. & M.3477. December, 1963.
5	M. V. Herbert R. J. Herd	Boundary-layer separation in supersonic propelling nozzles in the presence of external flow. A.R.C. R. & M.3421. August, 1964.
6	R. J. Herd G. T. Golesworthy	The performance of a centrebody propelling nozzle with a parallel shroud in external flow - Part I. A.R.C. C.P.841. November, 1963.
7	T. A. Cook	Some supersonic wind-tunnel tests on the fixing of boundary-layer transition using distributed roughness bands. R.A.E. (Bedford) Tech. Note Aero 2772. July, 1961.
8	J. C. Ascough	Tests on some convergent-divergent propelling nozzles with 6 in. diameter throats. Unpublished M.O.A. Report. 1964.

APPENDIX I

Notation

A	cross-sectional area
A*	isentropic nozzle throat area
A _g	geometric nozzle throat area
A _e	plane nozzle exit area
C _D	discharge coefficient (see Appendix II)
M _∞	external Mach number
P	static pressure
P _b	base pressure
P _t	model entry total pressure
P _w	wall static pressure
P _∞	ambient or free-stream static pressure
Q	mass flow
T _t	model entry total temperature
v	velocity
η _F	nozzle gross thrust efficiency (see Appendix II)
μ	throat vacuum thrust efficiency (see Appendix II)
φ	friction factor on supersonic expansion surfaces

Suffices

1	first ventilation slot
2	second ventilation slot
p	primary flow
sec	secondary flow

APPENDIX II

Definitions

E.P.R. = exhaust pressure ratio = $\frac{\text{nozzle entry total pressure}}{\text{ambient static pressure}} = \frac{P_t}{P_\infty}$

D.P.R. = design pressure ratio = that pressure ratio corresponding to the area ratio $\frac{A_e}{A_g}$ in one-dimensional theory

C_D = discharge coefficient = $\frac{\text{measured air mass flow}}{\text{isentropic air mass flow for the same physical throat area}} = \frac{\dot{A}^*}{A_g}$

= throat vacuum thrust efficiency = $\frac{\text{measured throat vacuum thrust with the nozzle choked}}{\text{isentropic throat vacuum thrust, passing the same mass flow}}$

η_F = nozzle gross thrust efficiency = $\frac{\text{measured thrust at given E.P.R.}}{\text{gauge thrust of an isentropic nozzle, passing the same mass flow, at the same E.P.R., when fully expanded}}$

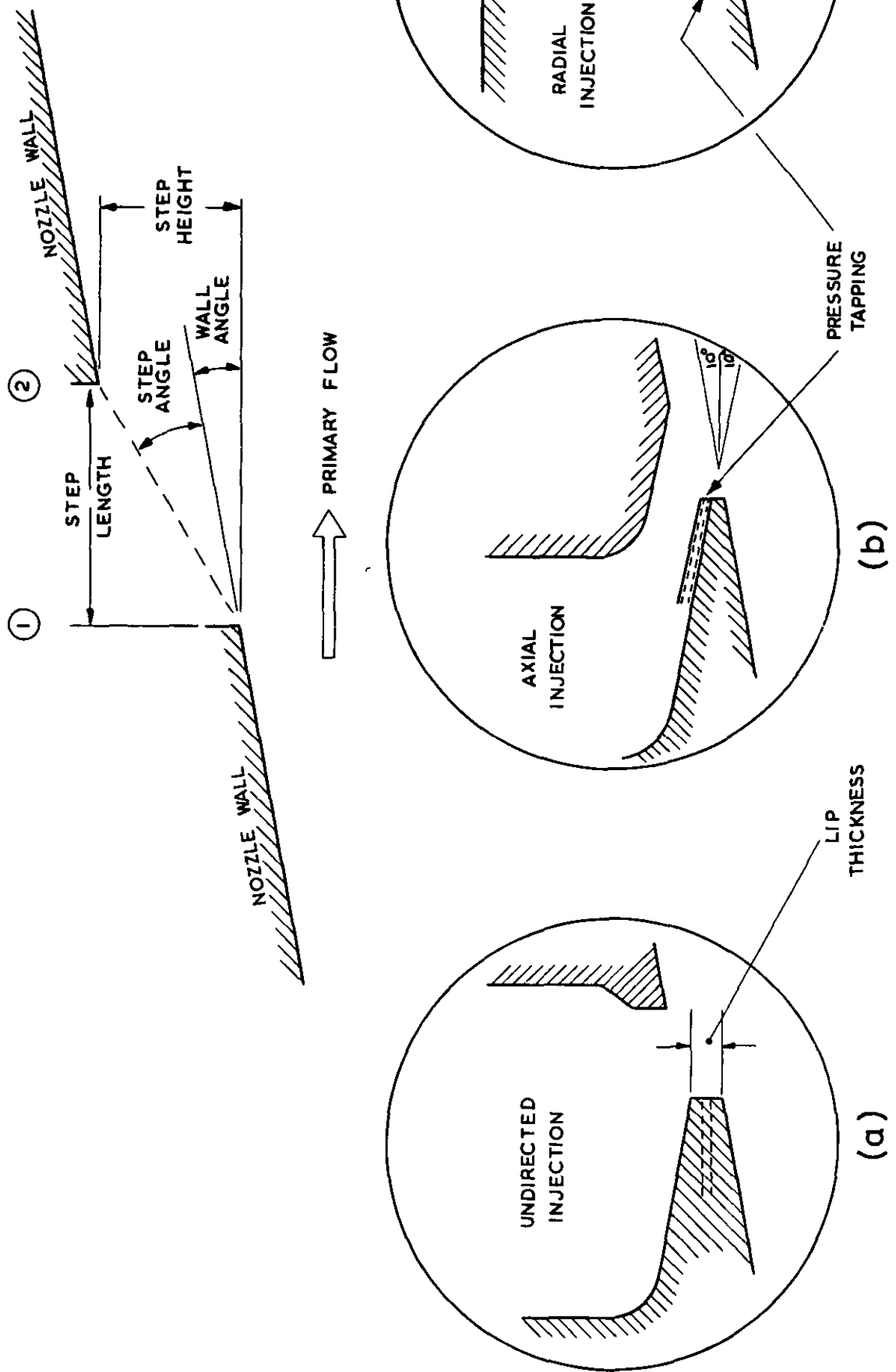
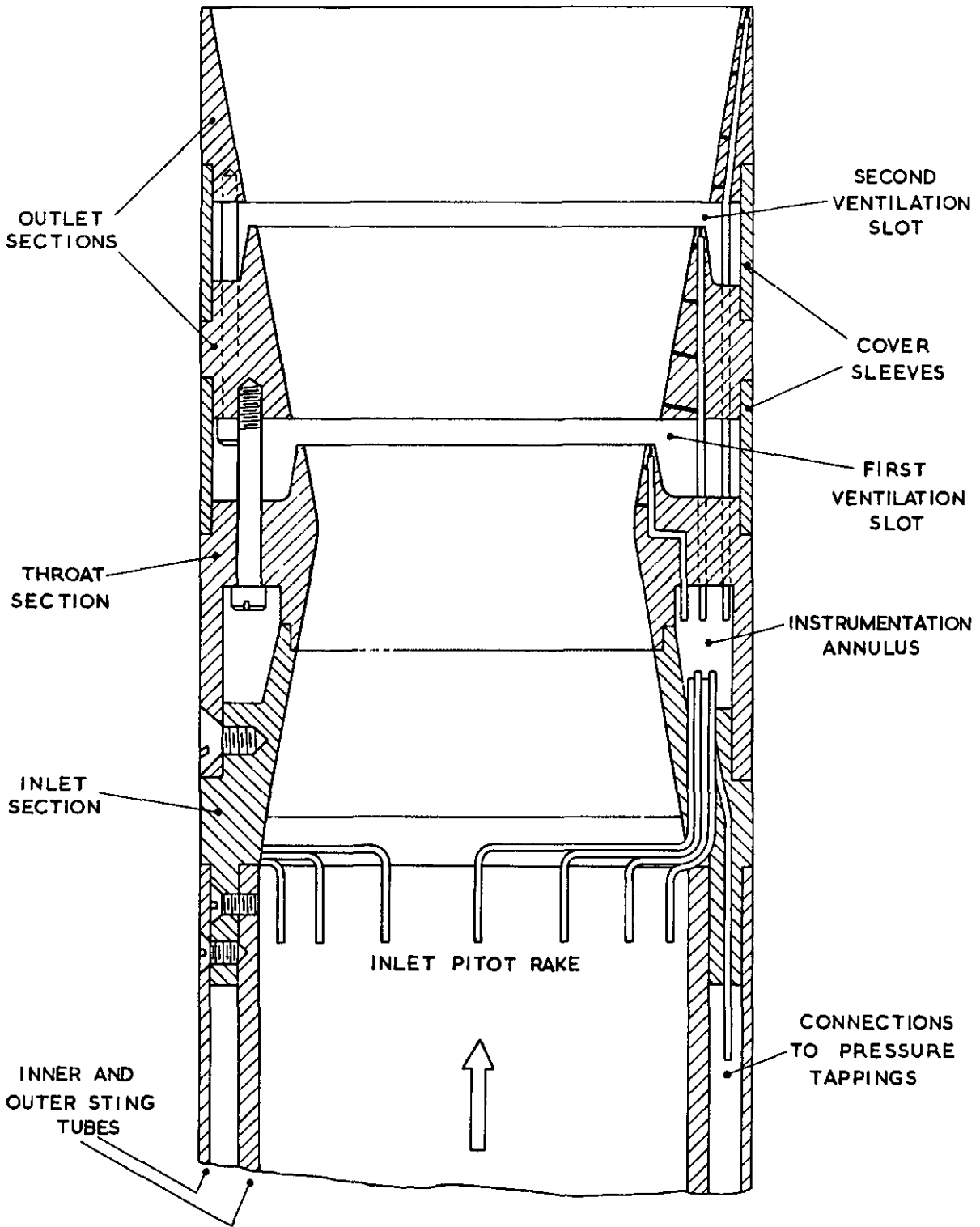


FIG. 1

VENTILATION SLOT GEOMETRY

FIG. 2

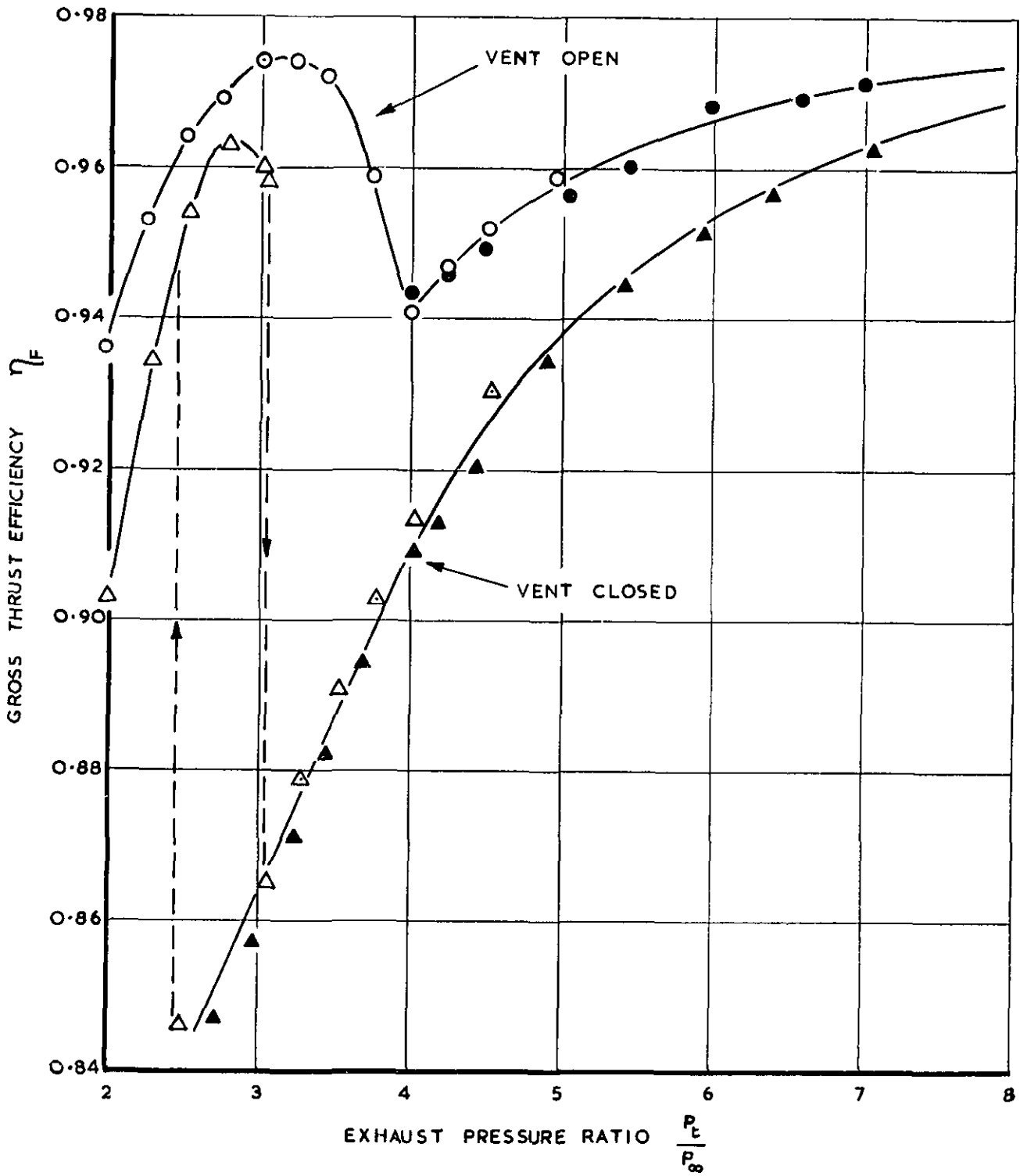


TWO-STAGE VENTILATED NOZZLE WITH UNDIRECTED INJECTION

ARRANGEMENT OF MODEL

SK 83055

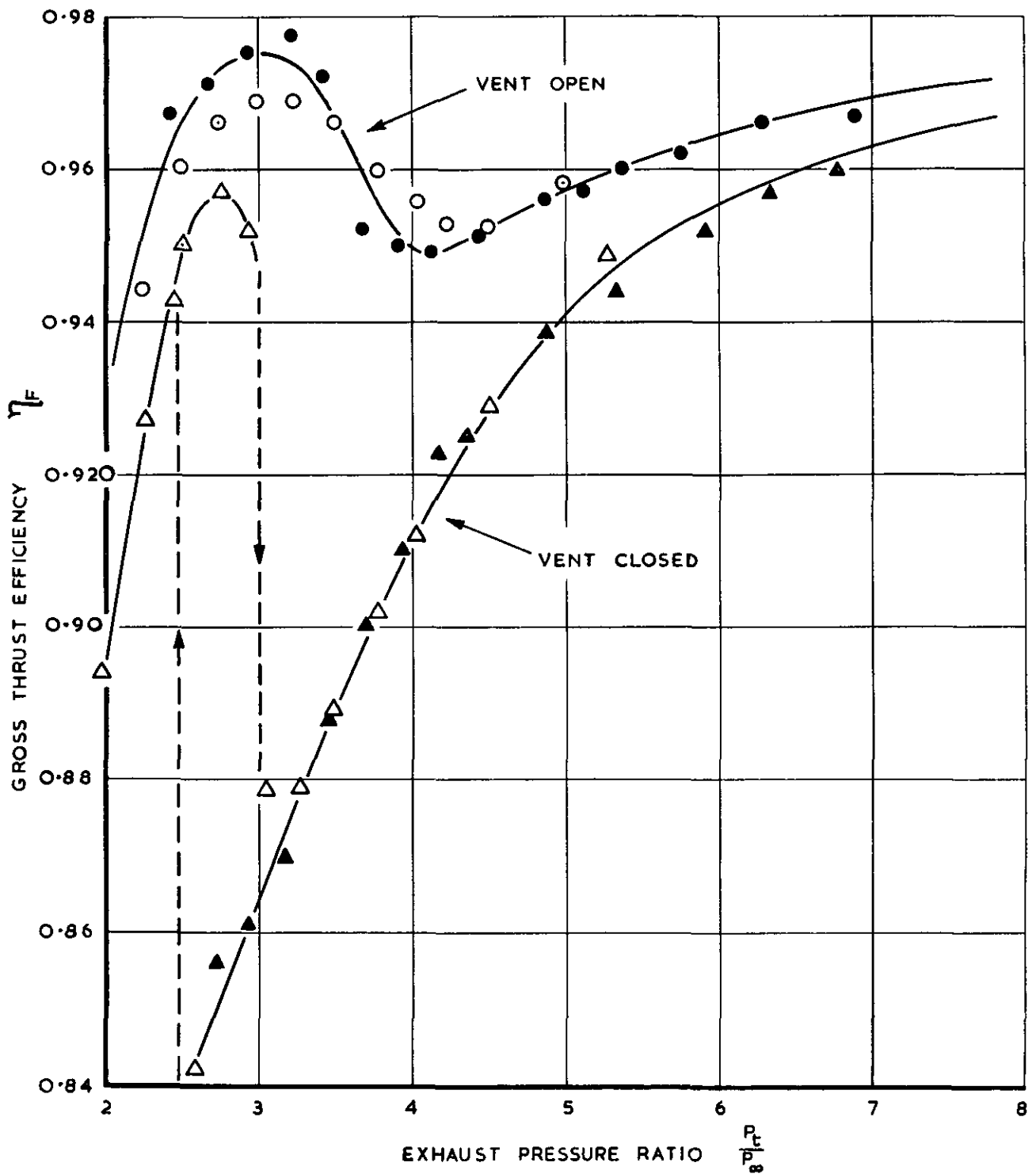
SINGLE-STAGE VENTILATED NOZZLE
 UNDIRECTED INJECTION
 NO ALLOWANCE FOR SECONDARY AIR DRAG
 D.P.R = 10 : $M_{\infty} = 0$
 FILLED SYMBOLS DENOTE THRUST RIG TESTS



SINGLE-STAGE NOZZLE EFFICIENCY IN QUIESCENT AIR

FIG. 4

SINGLE-STAGE VENTILATED NOZZLE
AXIAL INJECTION
NO ALLOWANCE FOR SECONDARY AIR DRAG
D.P.R = 10 : $M_b = 0$
FILLED SYMBOLS DENOTE THRUST RIG TESTS



SINGLE-STAGE NOZZLE EFFICIENCY IN QUIESCENT AIR

SK 83057

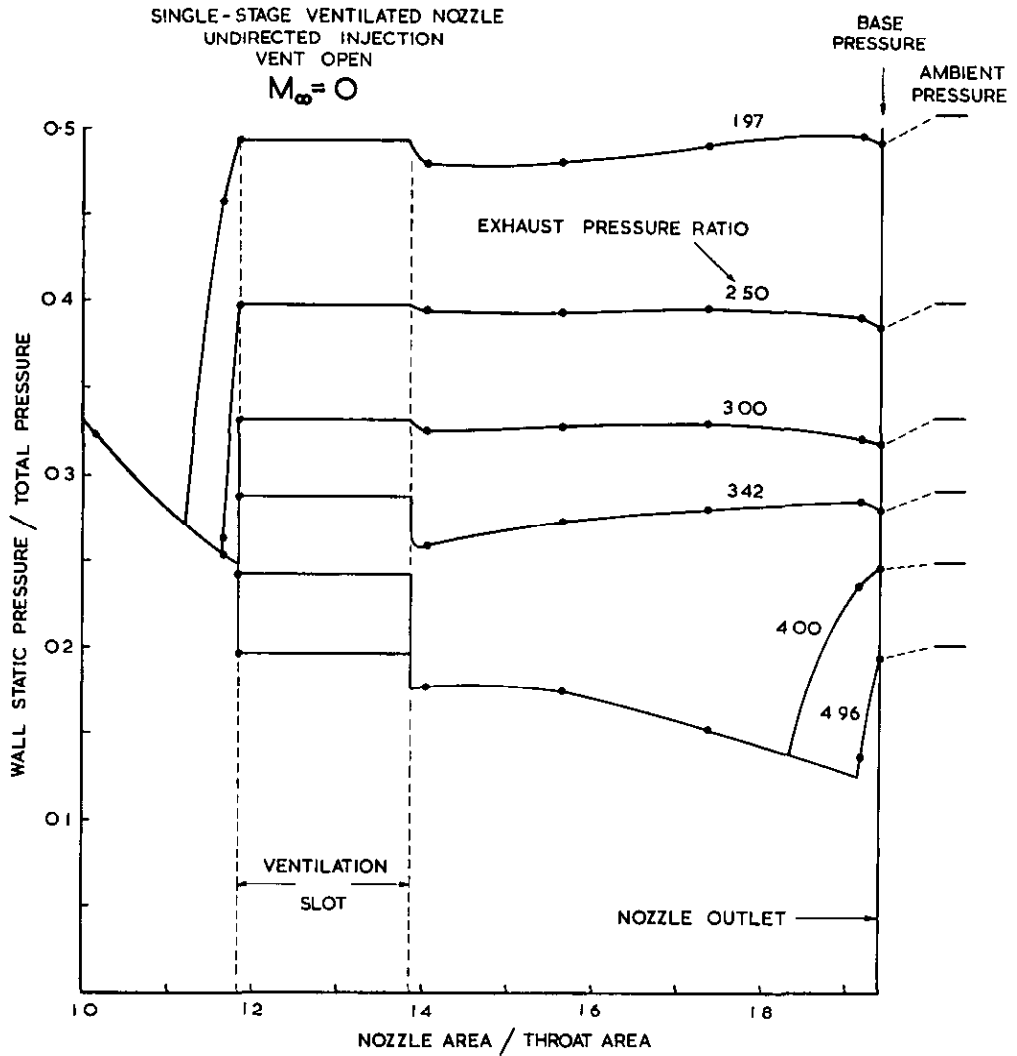


FIG.5

SINGLE-STAGE NOZZLE PRESSURE DISTRIBUTION

SK 83058

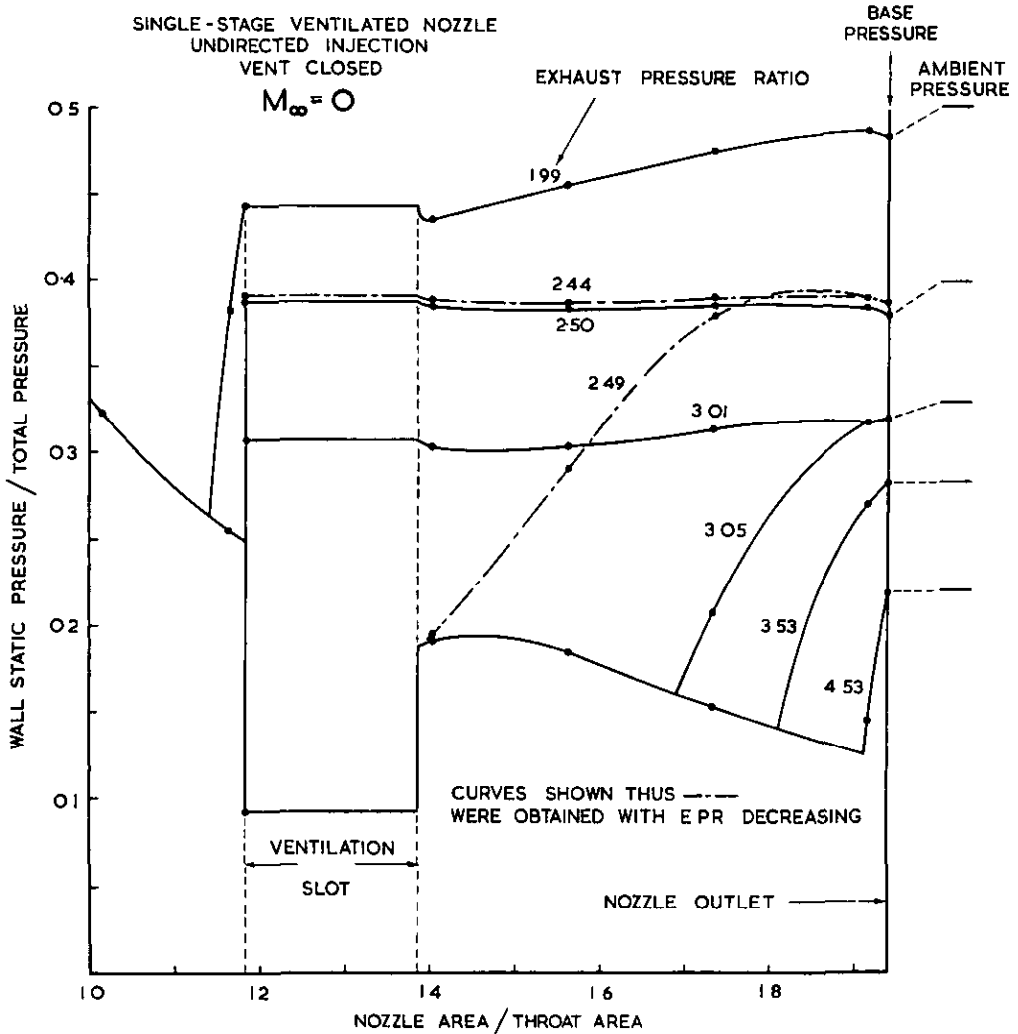


FIG.6

SINGLE-STAGE NOZZLE PRESSURE DISTRIBUTION

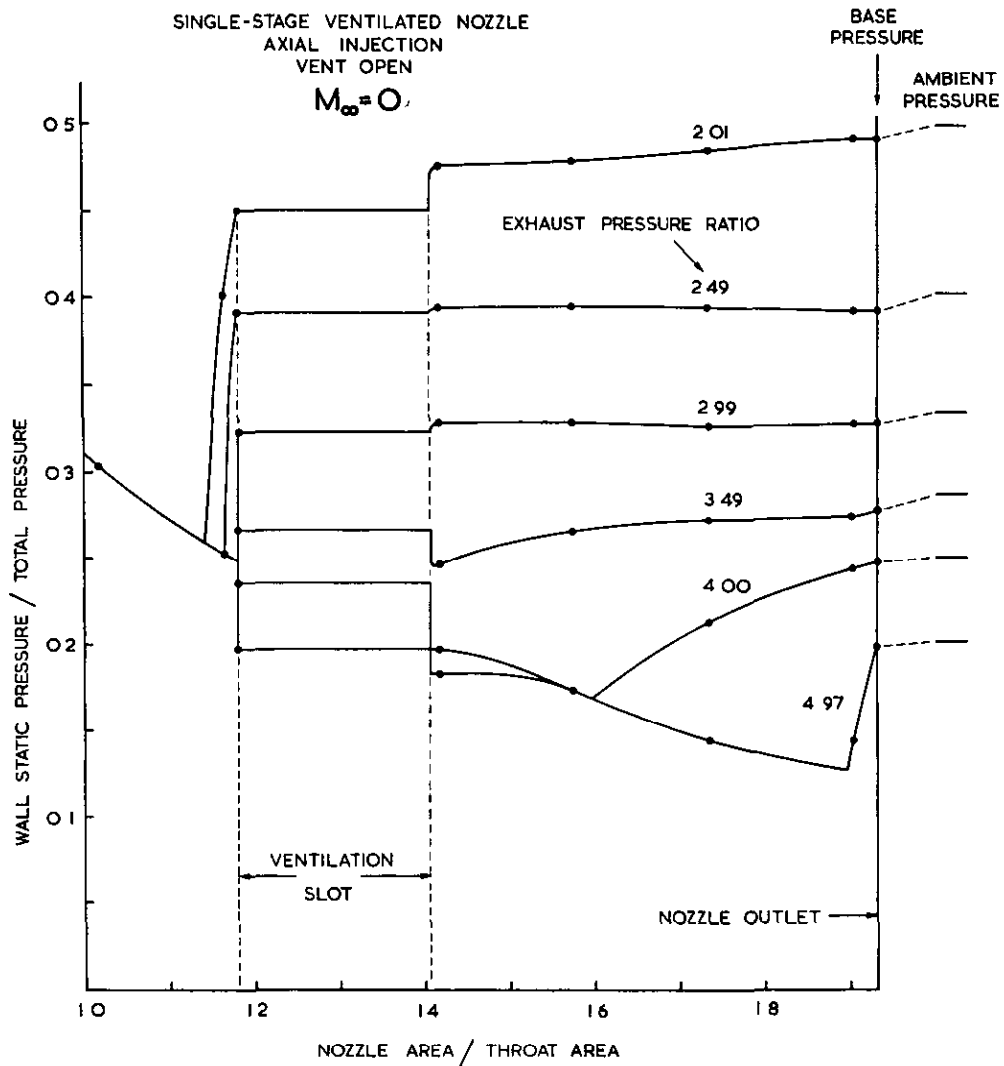


FIG.7

SINGLE-STAGE NOZZLE PRESSURE DISTRIBUTION

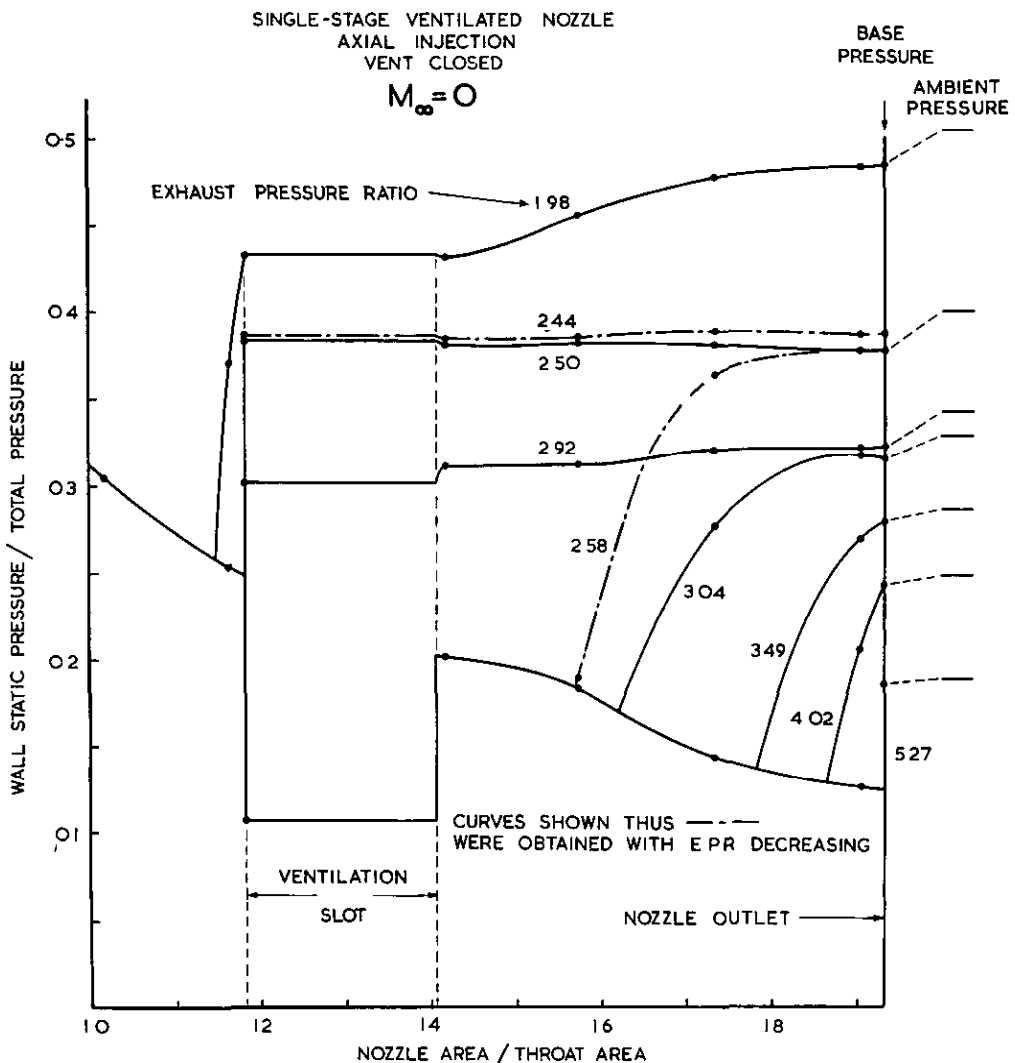
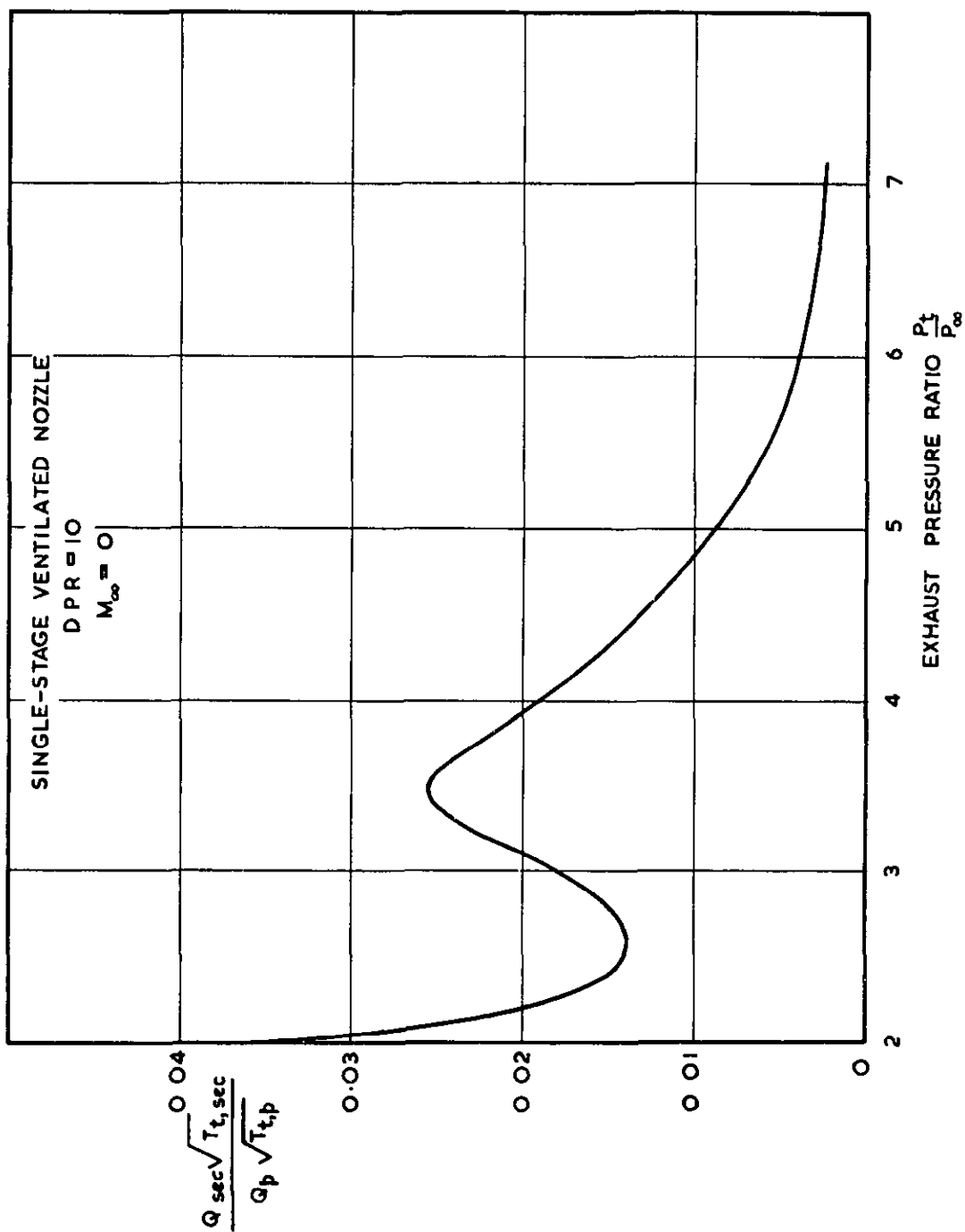


FIG.8

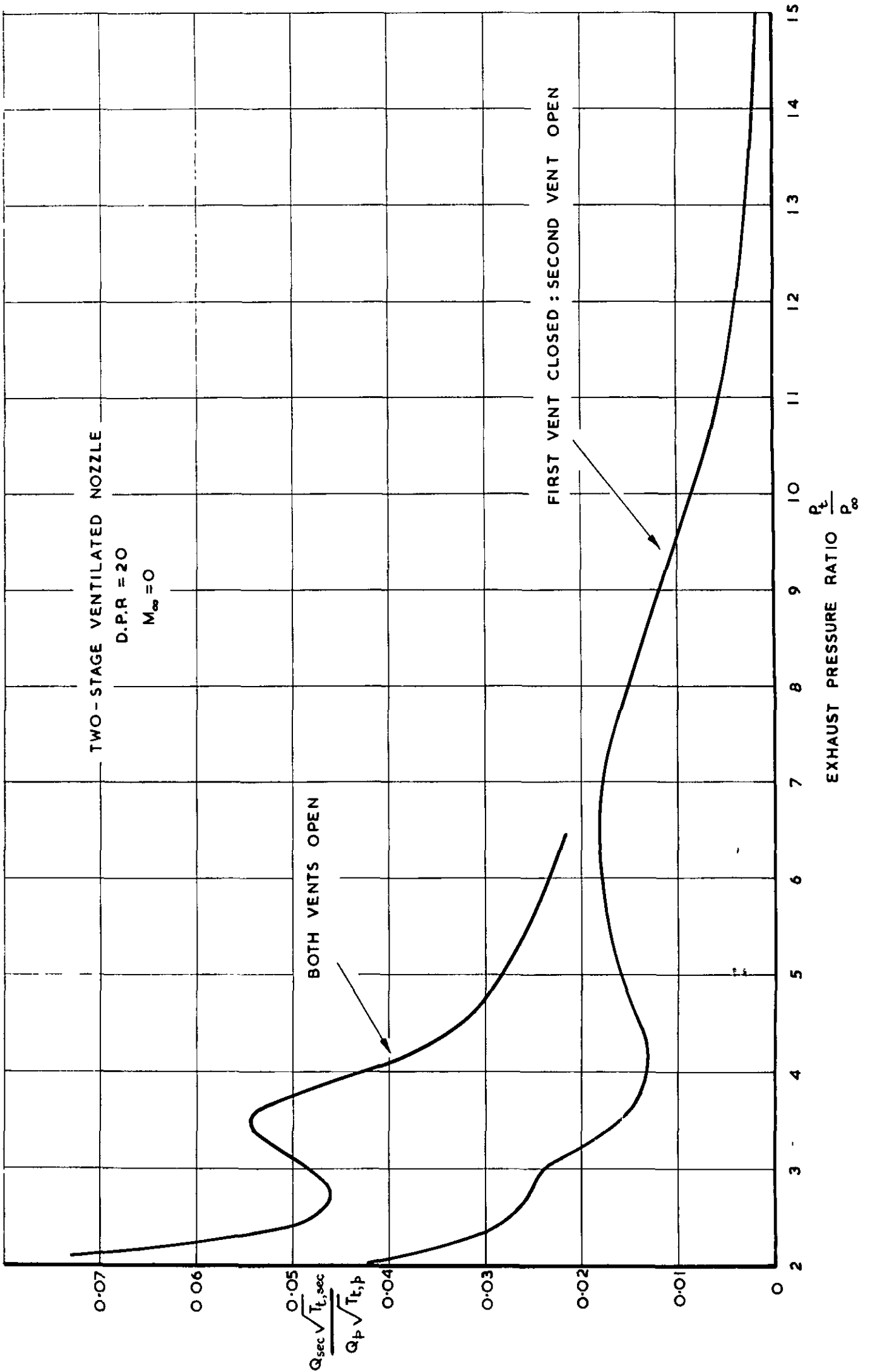
SINGLE-STAGE NOZZLE PRESSURE DISTRIBUTION

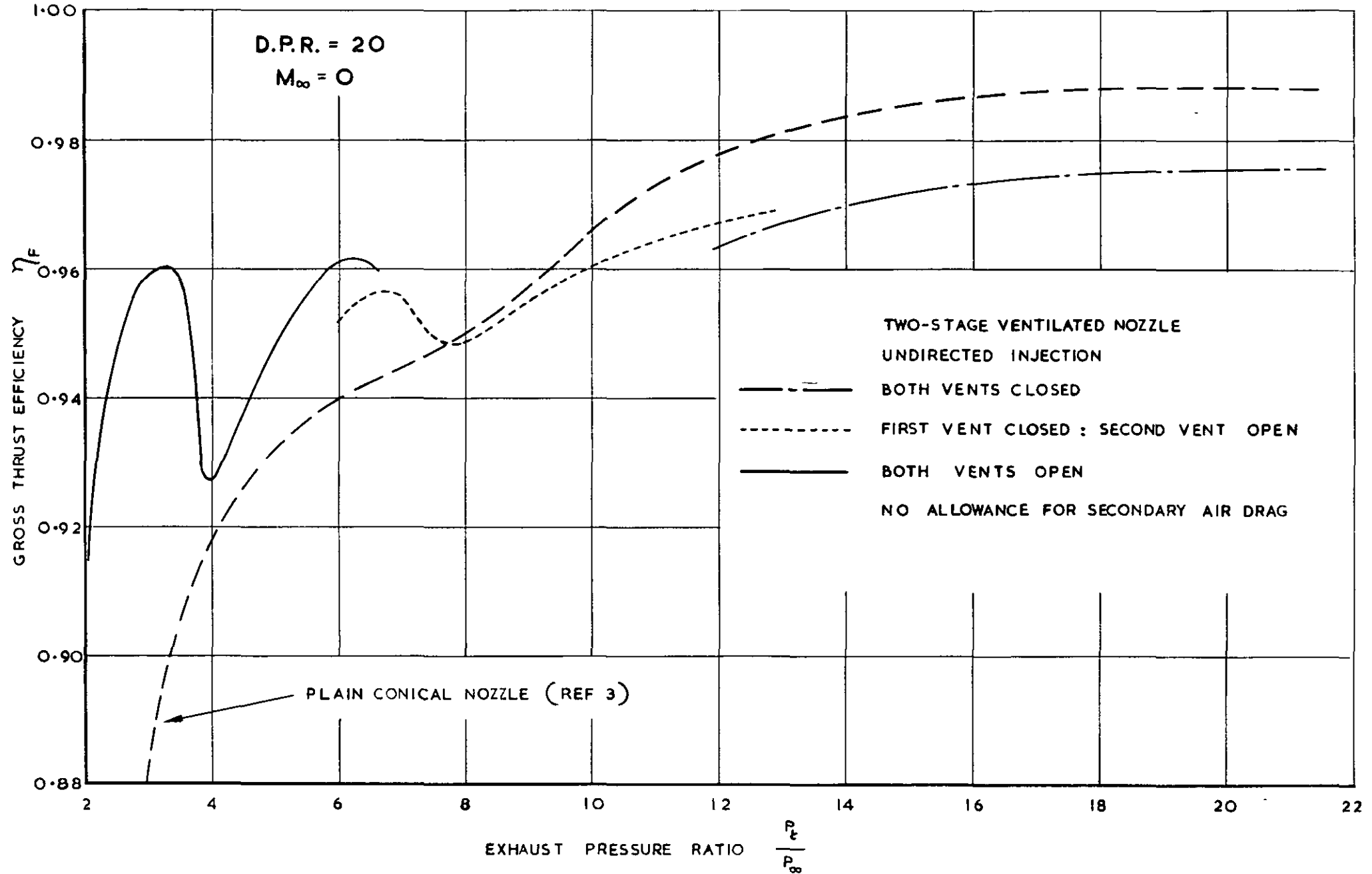


SECONDARY MASS FLOW

FIG. 9

FIG. 10





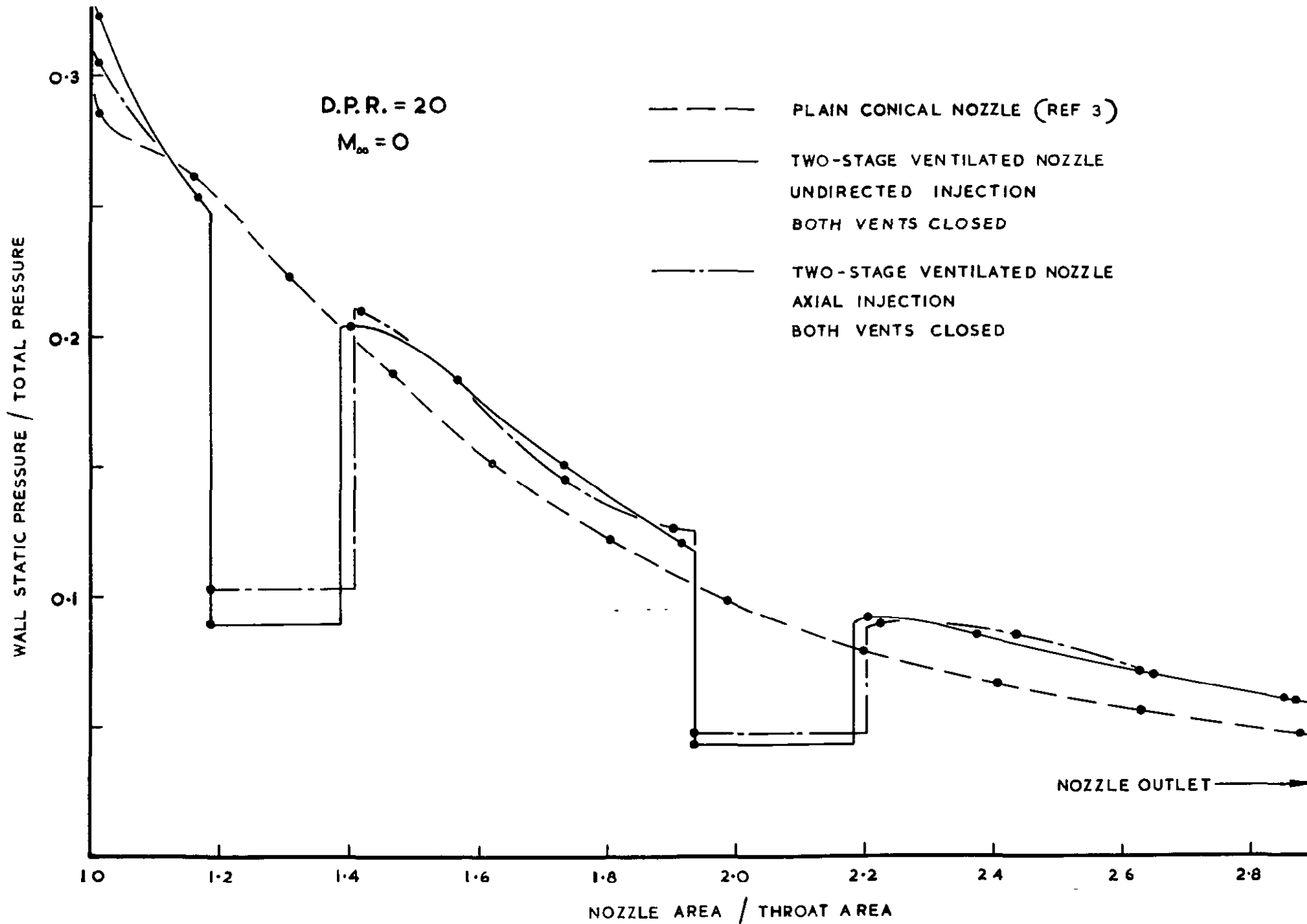
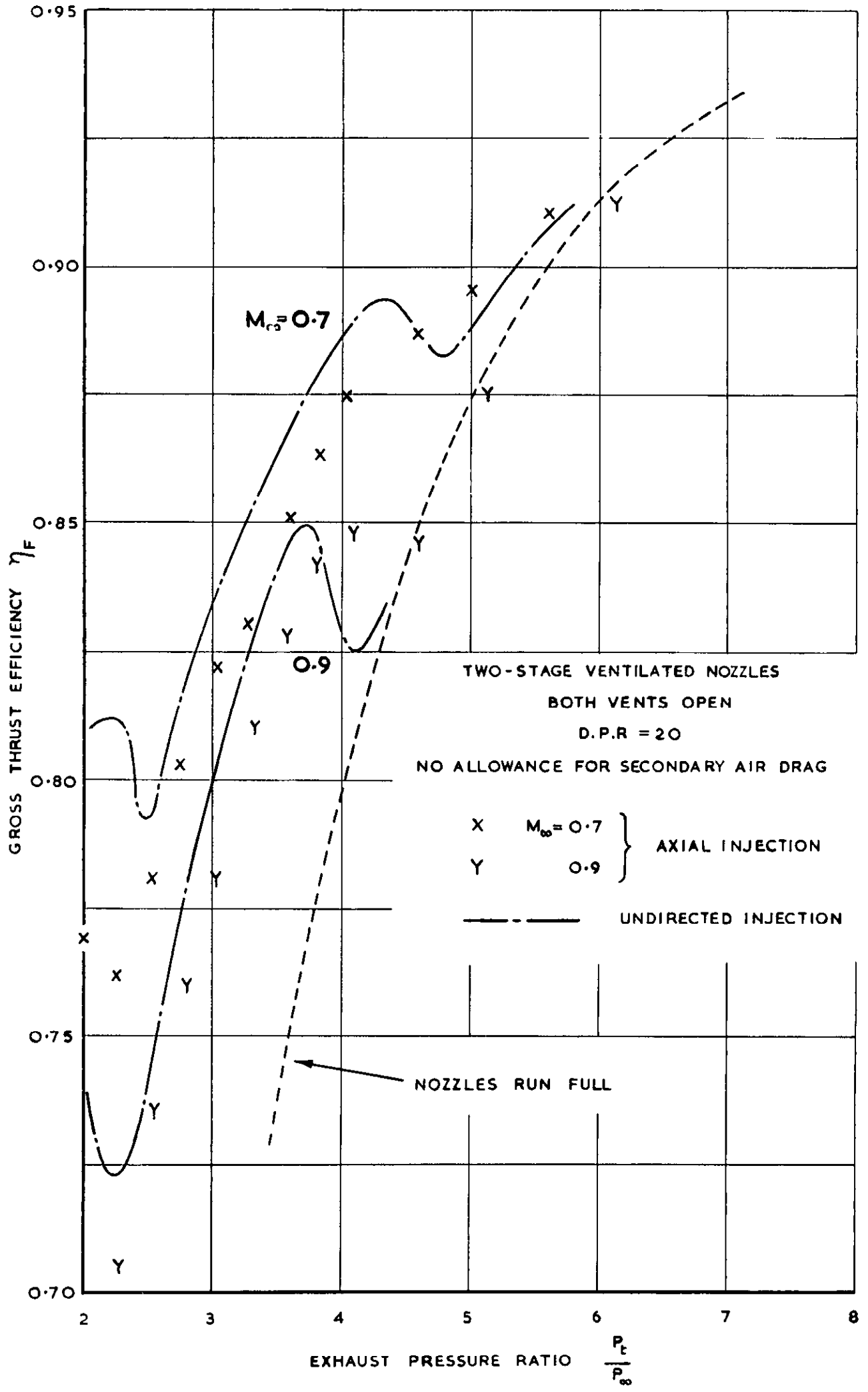


FIG.14

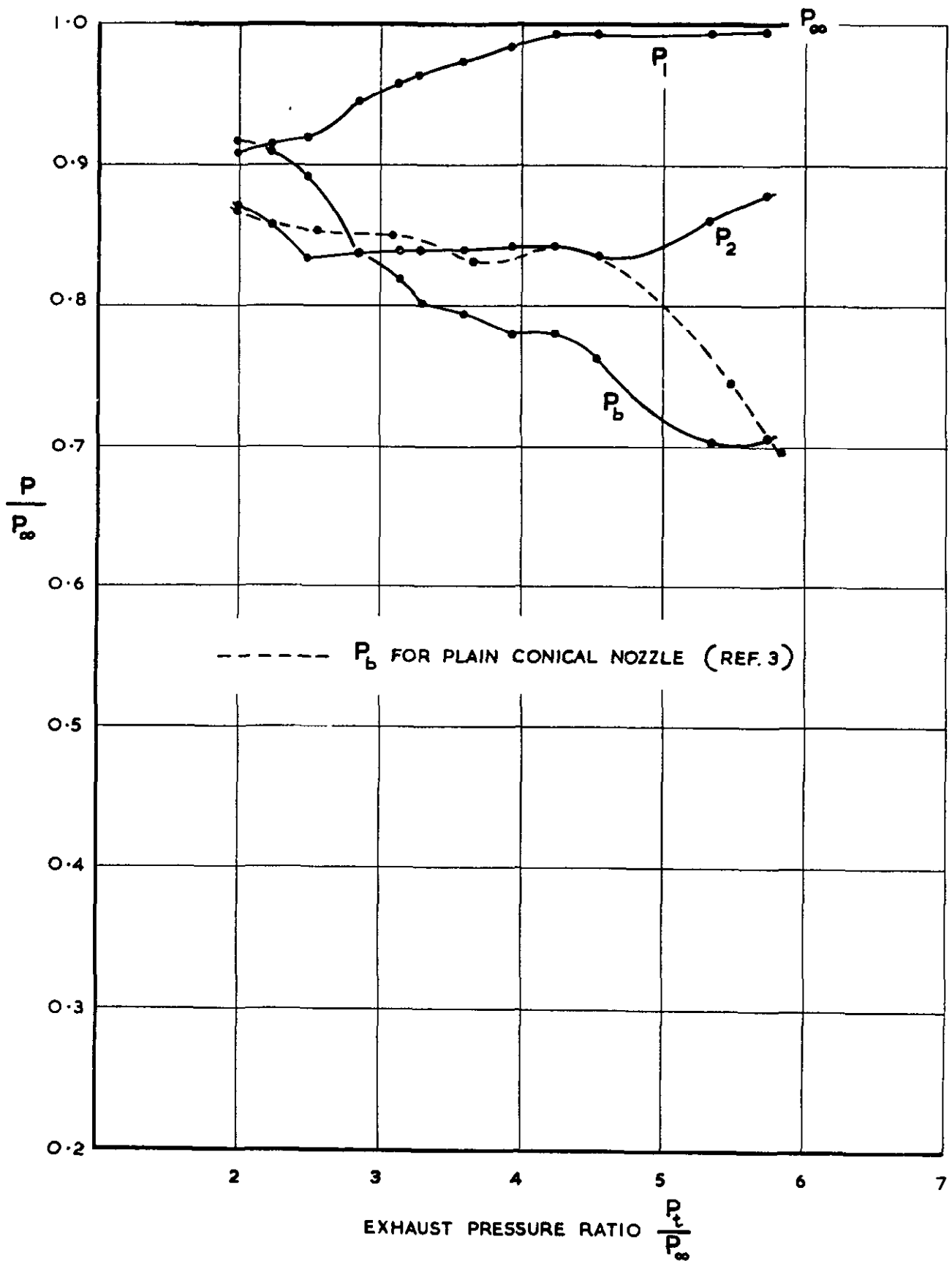


TWO-STAGE NOZZLE EFFICIENCY IN EXTERNAL FLOW

FIG.18a

TWO-STAGE VENTILATED NOZZLE
 UNDIRECTED INJECTION
 BOTH VENTS OPEN

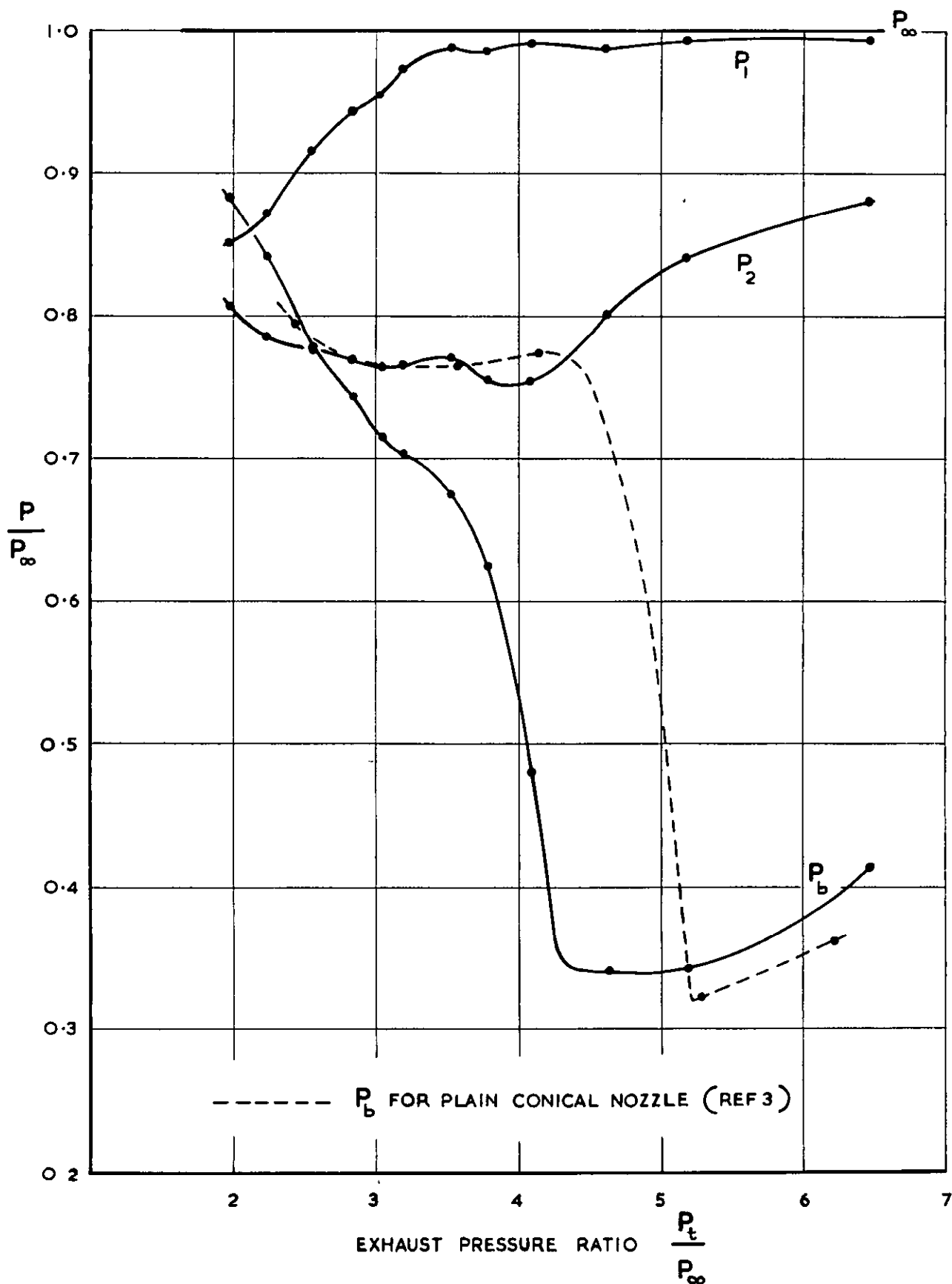
$M_\infty = 0.7$



VENTILATION SLOT PRESSURES

TWO-STAGE VENTILATED NOZZLE
 UNDIRECTED INJECTION
 BOTH VENTS OPEN

$M_\infty = 0.9$

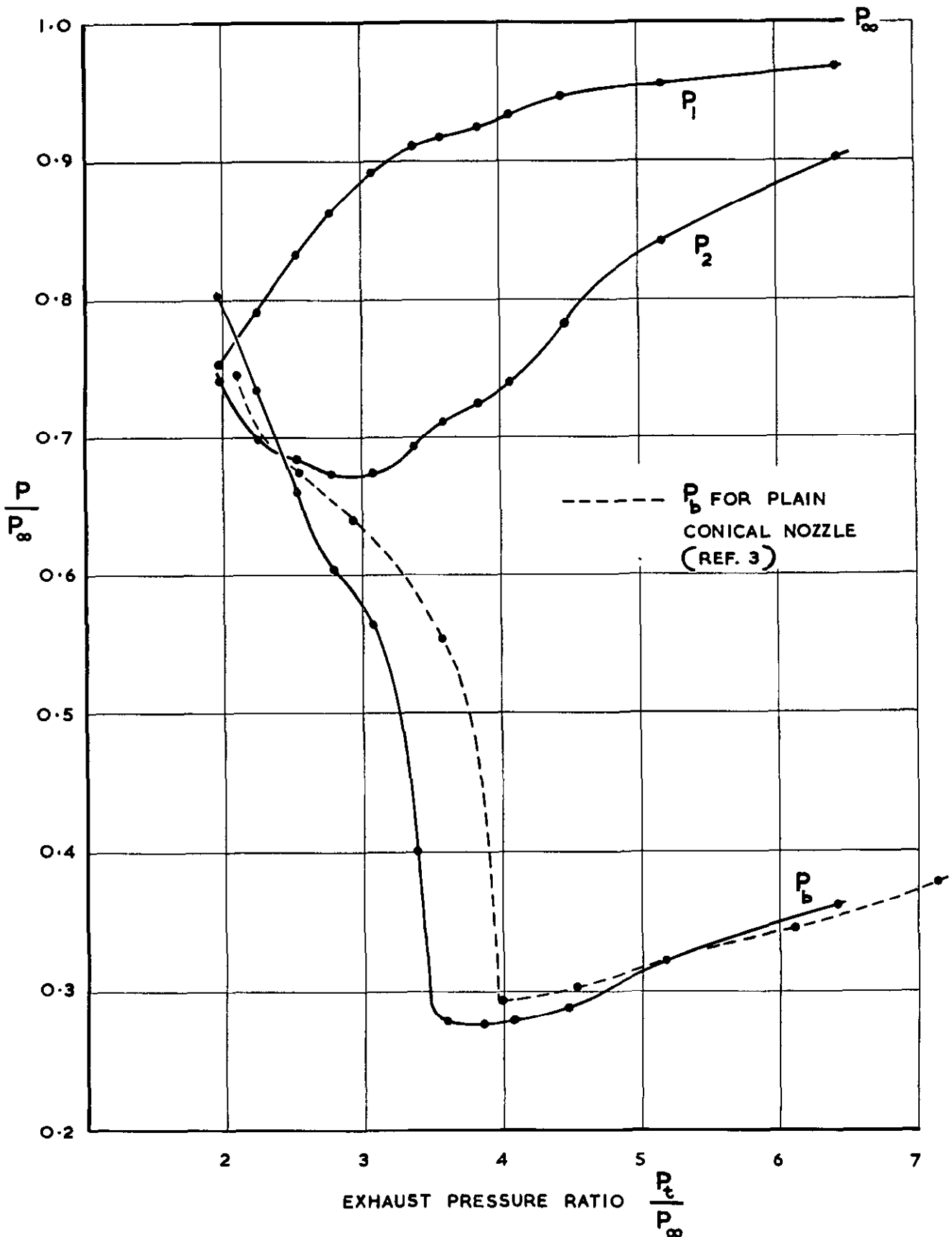


VENTILATION SLOT PRESSURES

SK 83071

**TWO-STAGE VENTILATED NOZZLE
UNDIRECTED INJECTION
BOTH VENTS OPEN**

$M_\infty = 1.1$

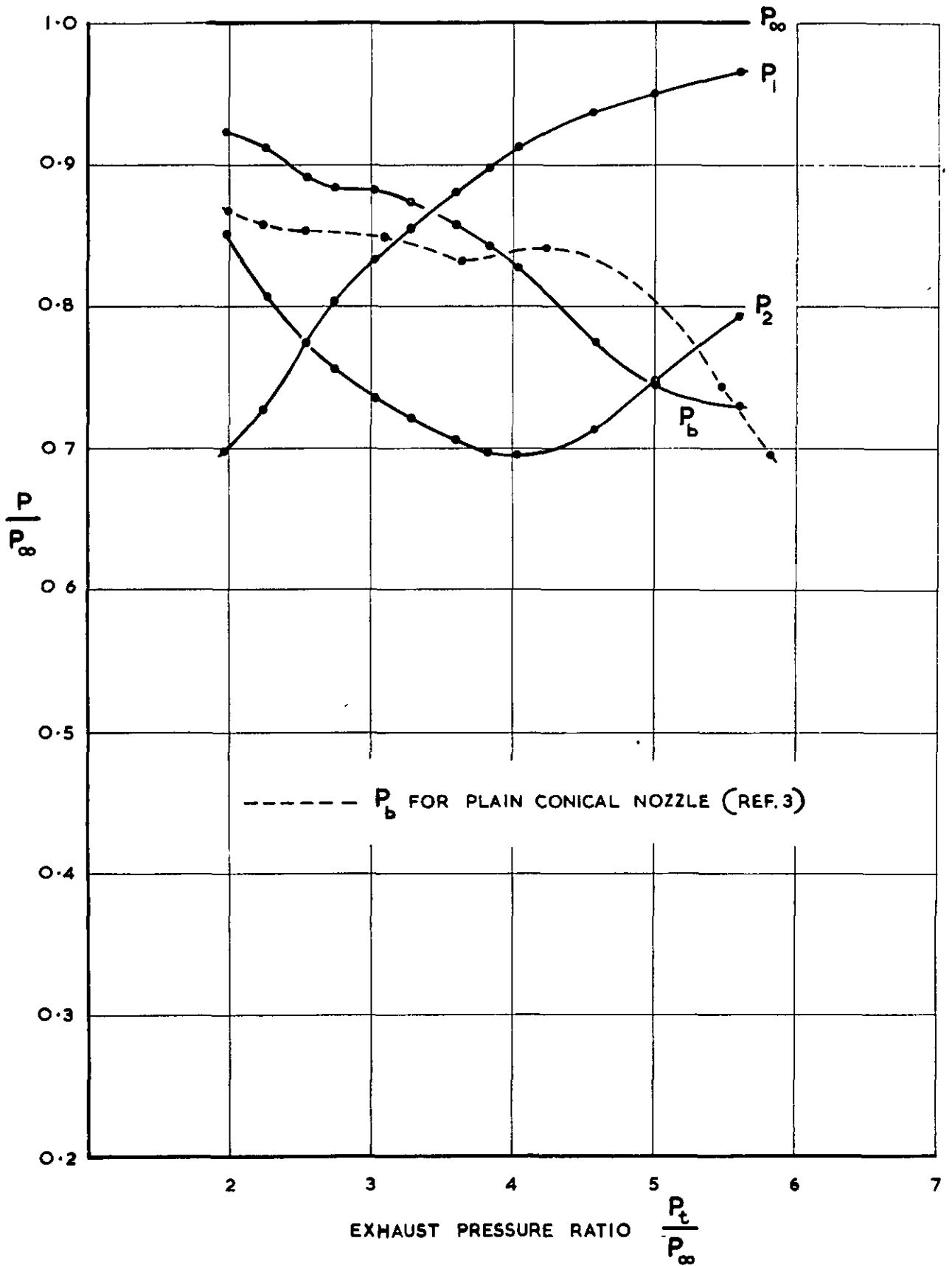


VENTILATION SLOT PRESSURES

SK 83075

TWO-STAGE VENTILATED NOZZLE
 AXIAL INJECTION
 BOTH VENTS OPEN

$$M_{\infty} = 0.7$$

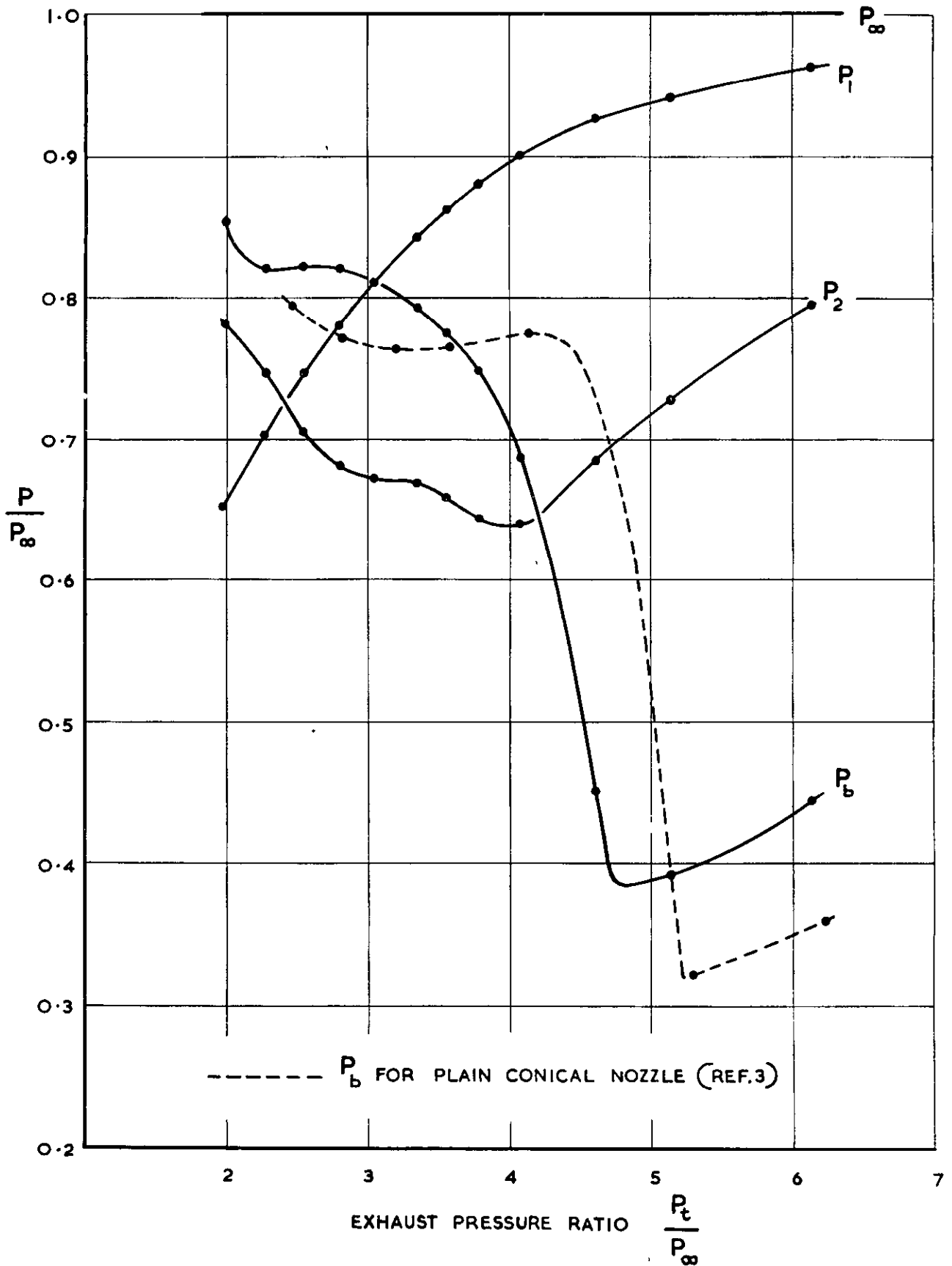


VENTILATION SLOT PRESSURES

FIG.19b

TWO-STAGE VENTILATED NOZZLE
AXIAL INJECTION
BOTH VENTS OPEN

$$M_{\infty} = 0.9$$



VENTILATION SLOT PRESSURES

SK 83077

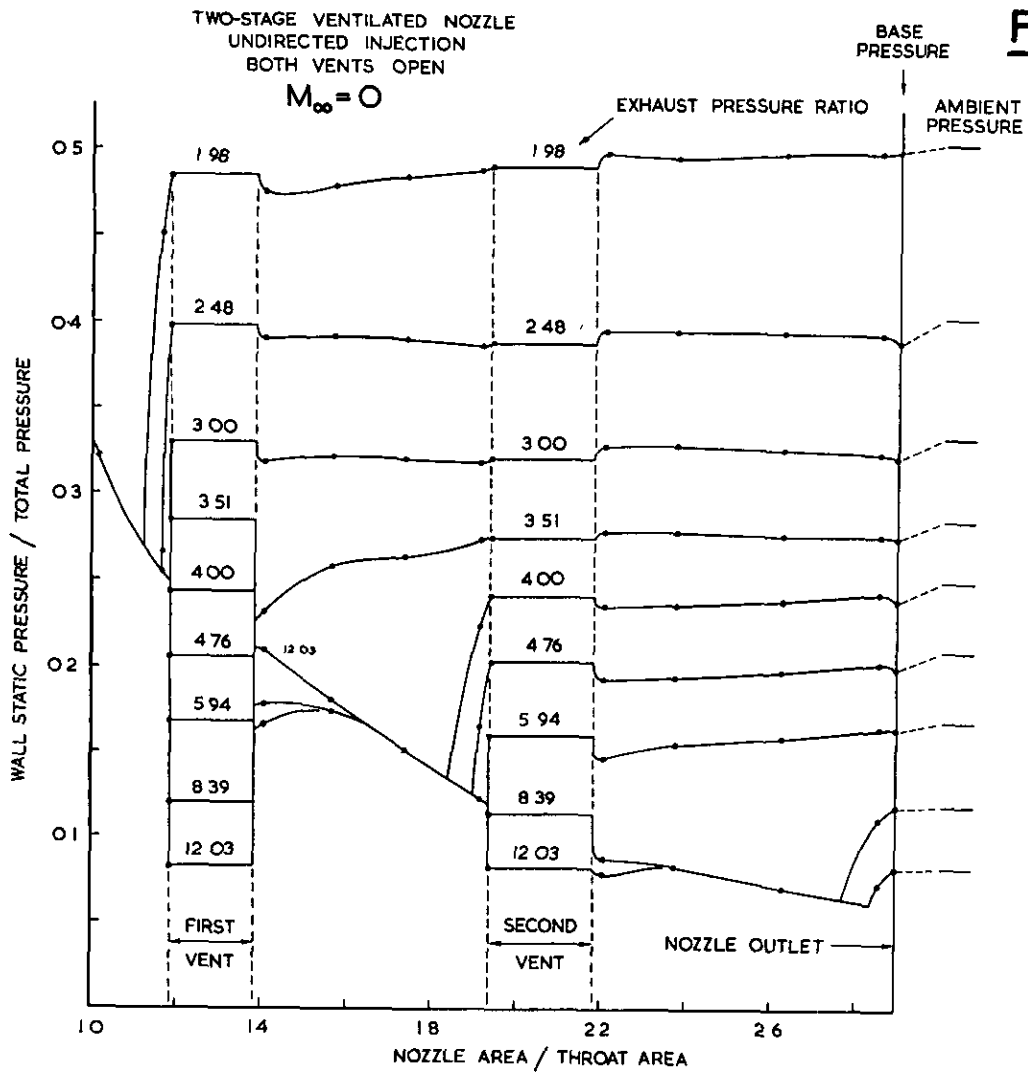


FIG. 20a

TWO-STAGE NOZZLE PRESSURE DISTRIBUTION

SK 83078

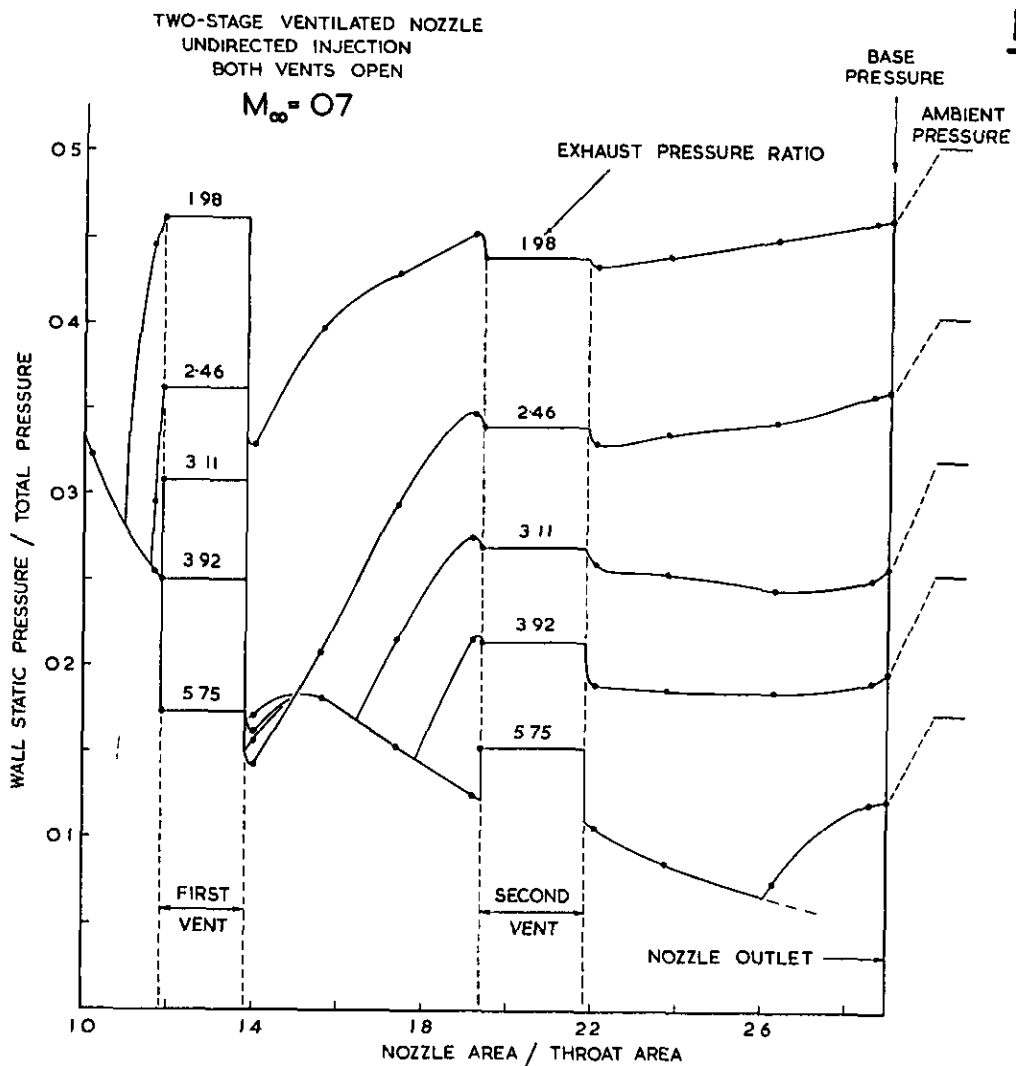
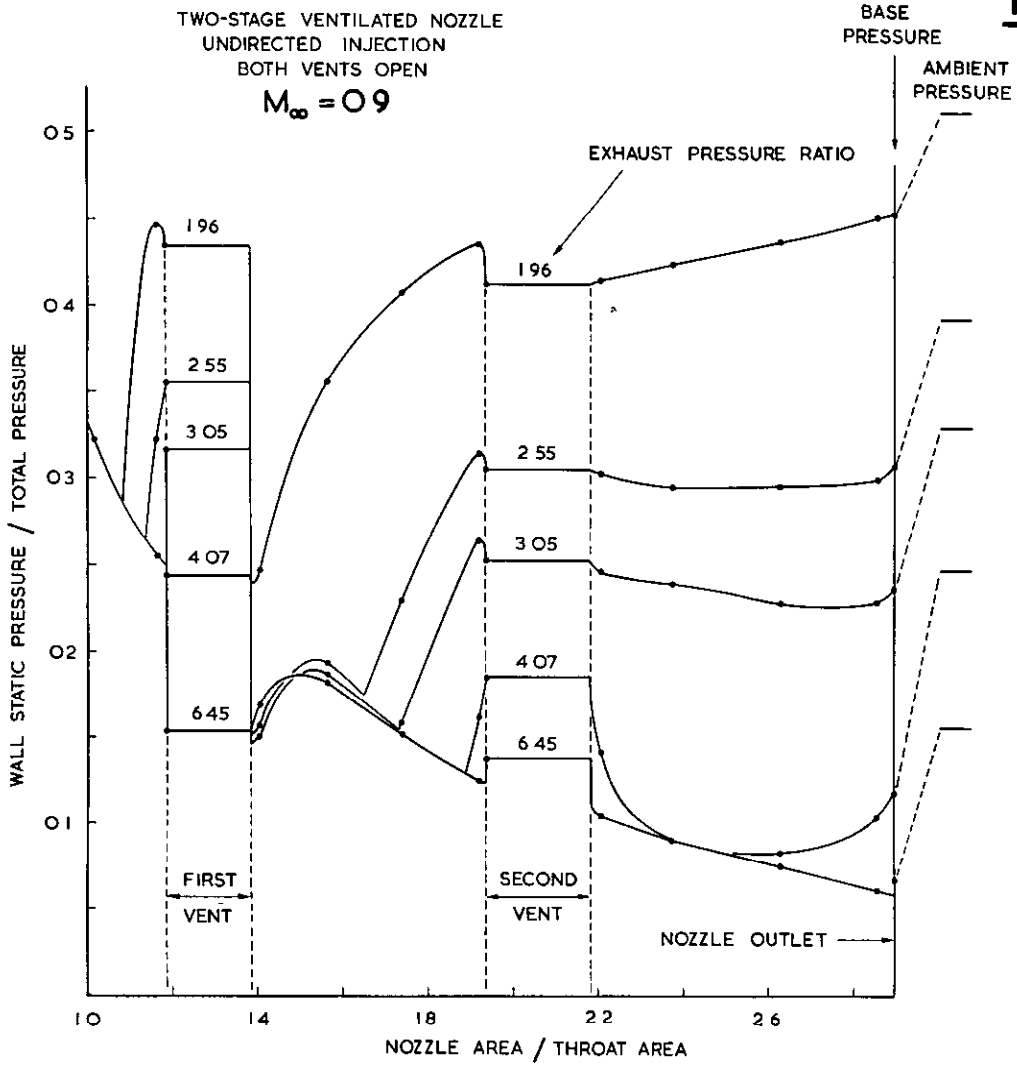
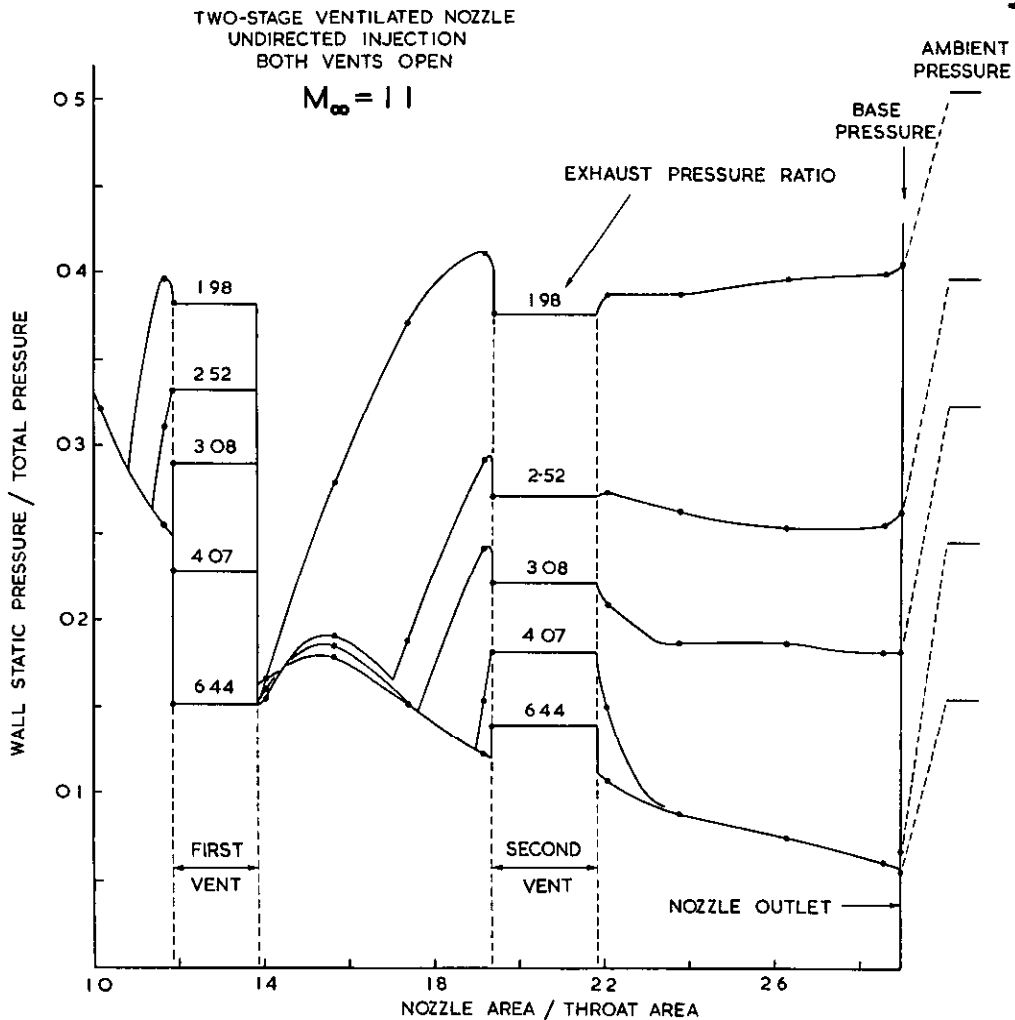


FIG. 20b

TWO-STAGE NOZZLE PRESSURE DISTRIBUTION



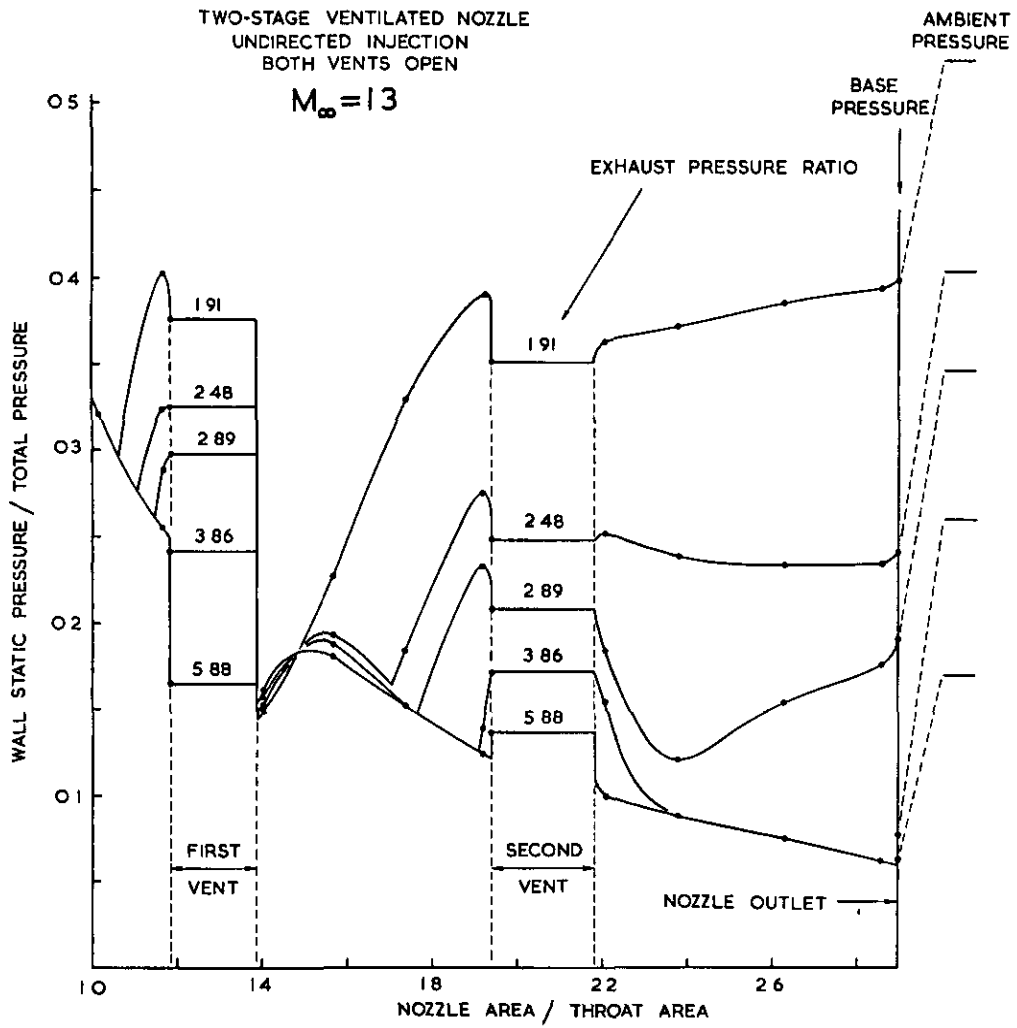
TWO-STAGE NOZZLE PRESSURE DISTRIBUTION



TWO-STAGE NOZZLE PRESSURE DISTRIBUTION

SK 83081

FIG.20e



TWO-STAGE NOZZLE PRESSURE DISTRIBUTION

SK 83082

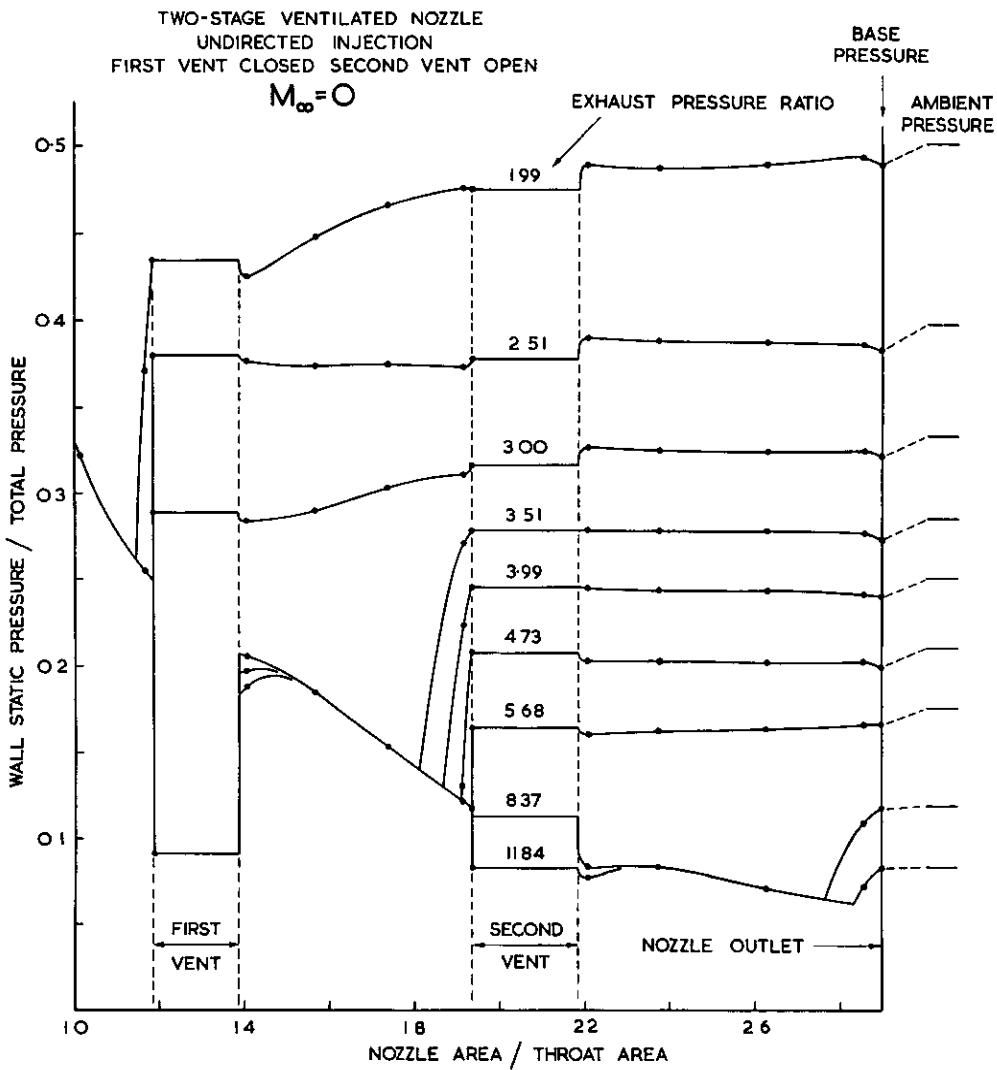


FIG. 21a

TWO-STAGE NOZZLE PRESSURE DISTRIBUTION

SK 83083

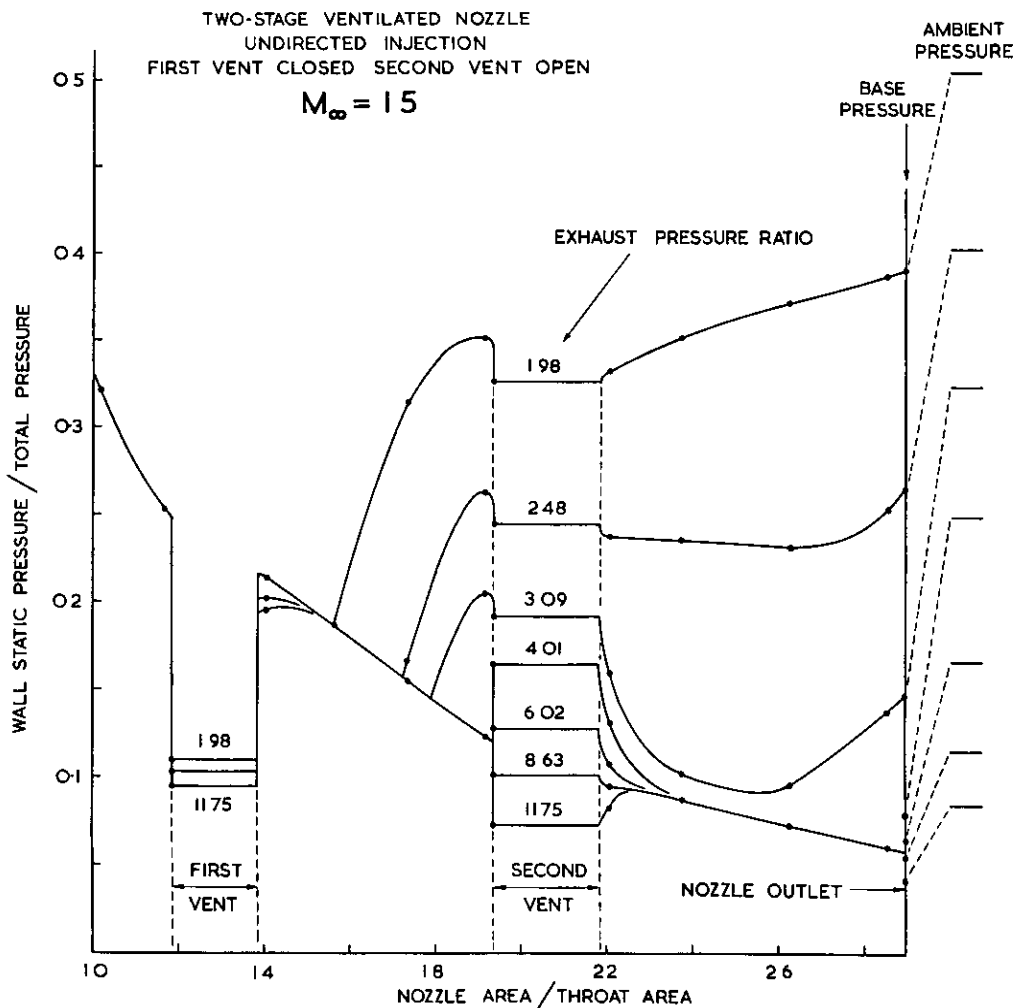


FIG. 21 b

TWO-STAGE NOZZLE PRESSURE DISTRIBUTION

SK 83084

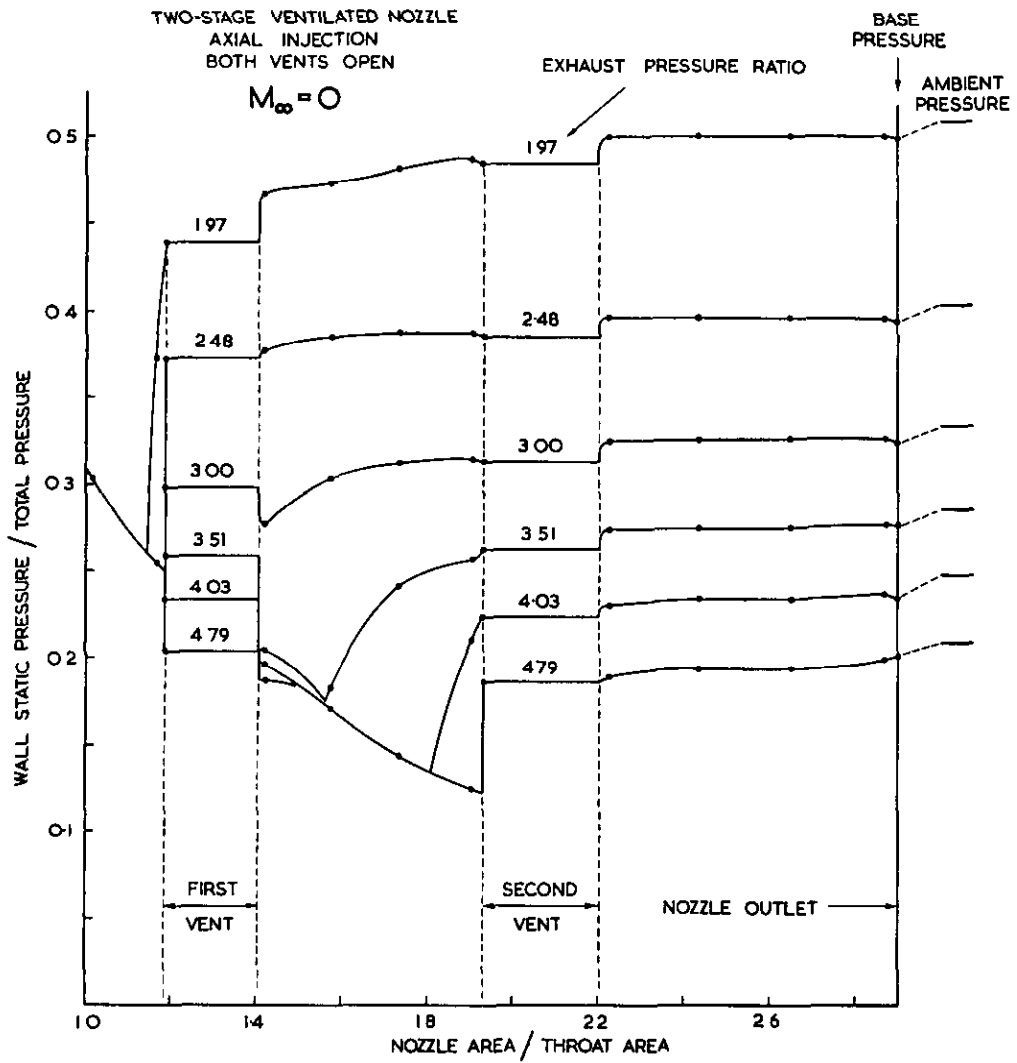


FIG.22

TWO-STAGE NOZZLE PRESSURE DISTRIBUTION

SK 83085

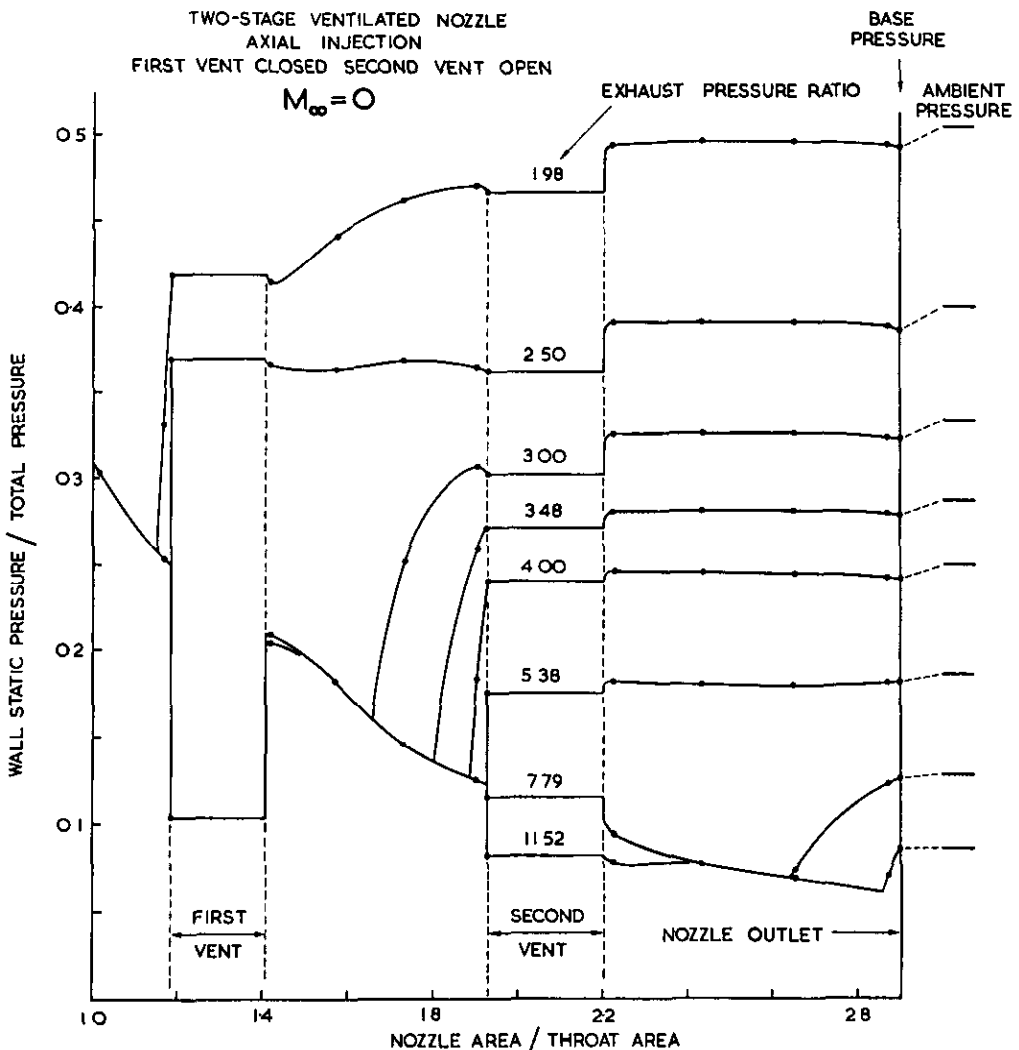


FIG.23

TWO-STAGE NOZZLE PRESSURE DISTRIBUTION

TWO-STAGE NOZZLE PRESSURE DISTRIBUTION

TWO-STAGE VENTILATED NOZZLE
 UNDIRECTED INJECTION
 BOTH VENTS OPEN

E.P.R. = 3.0

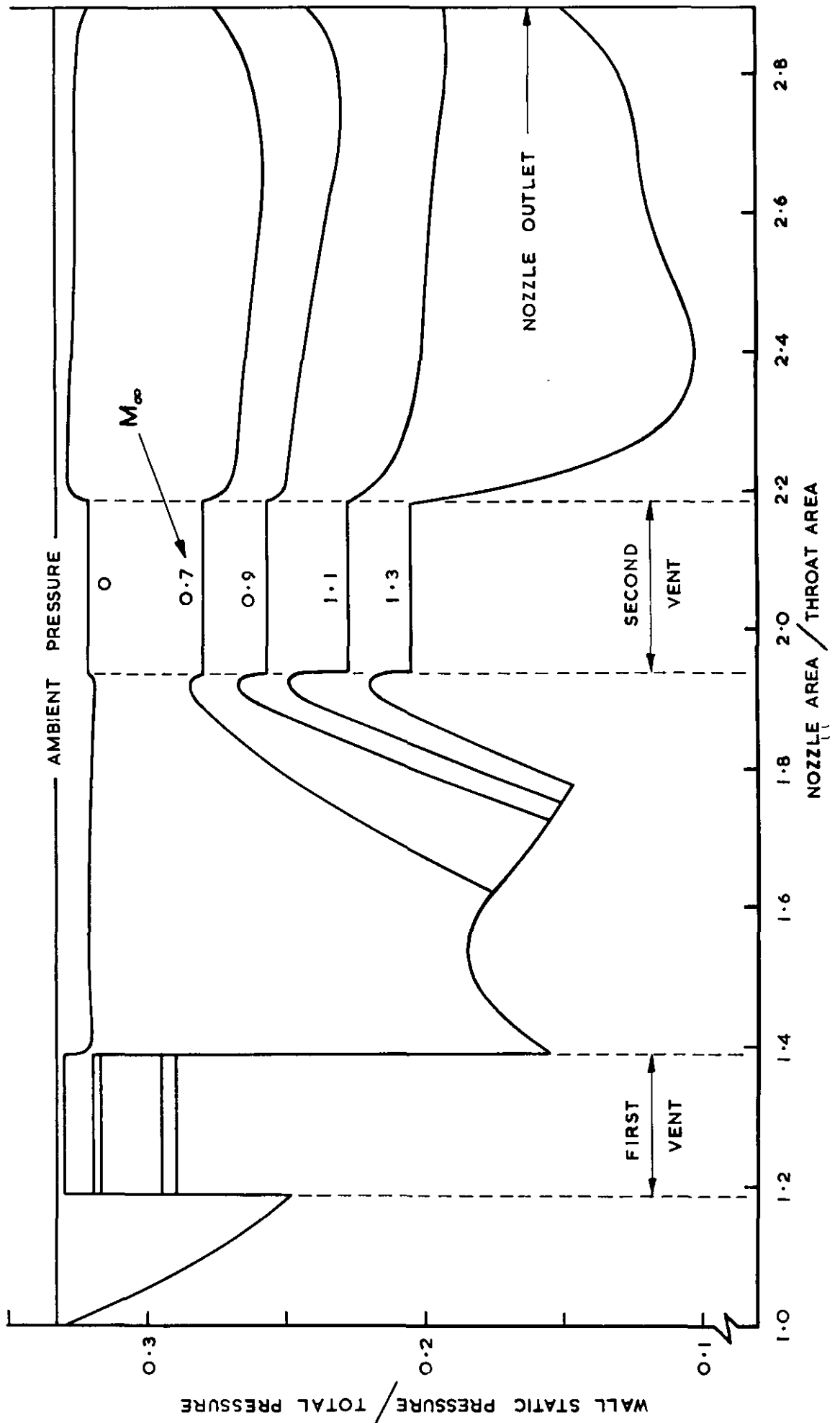
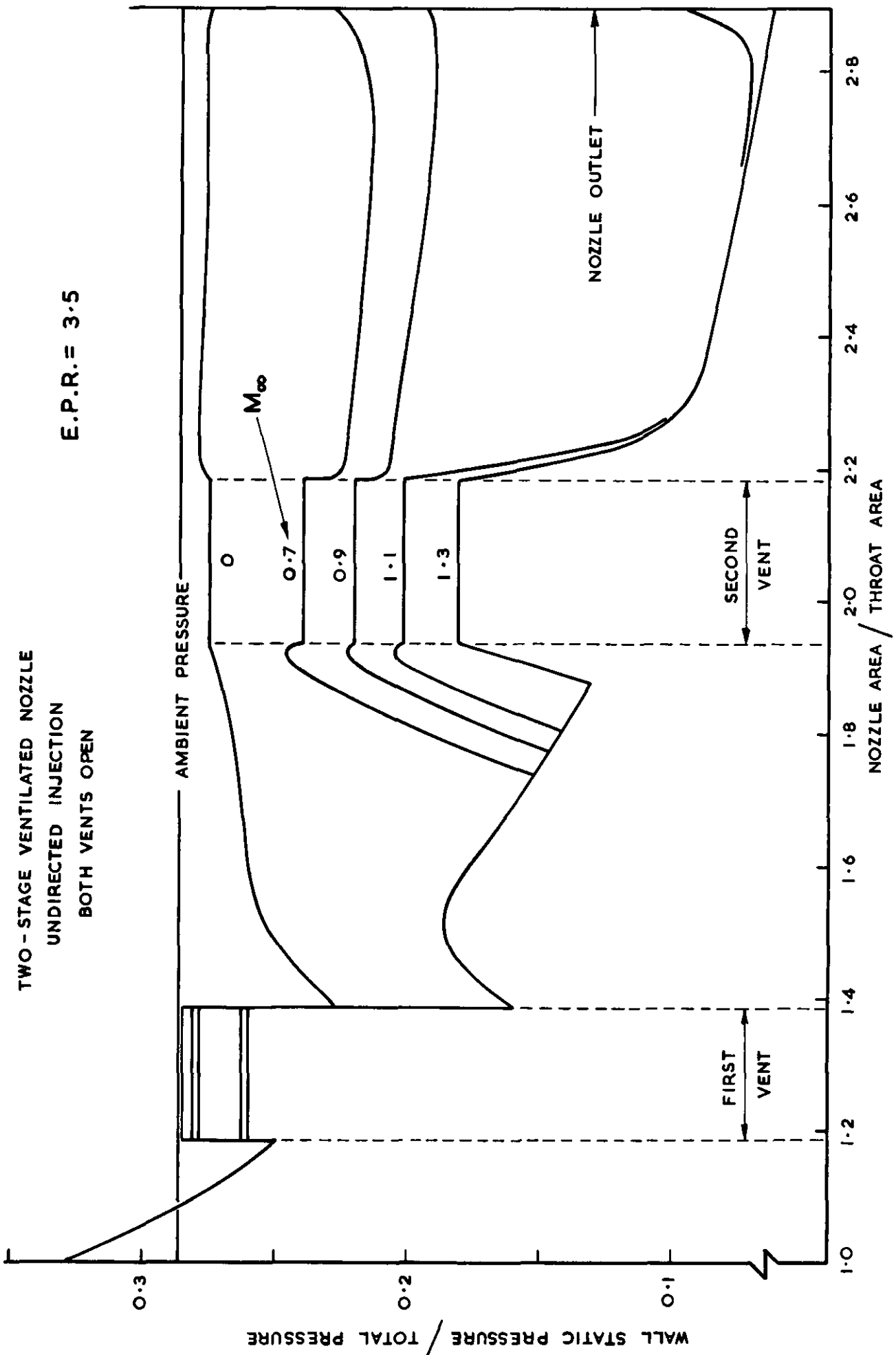
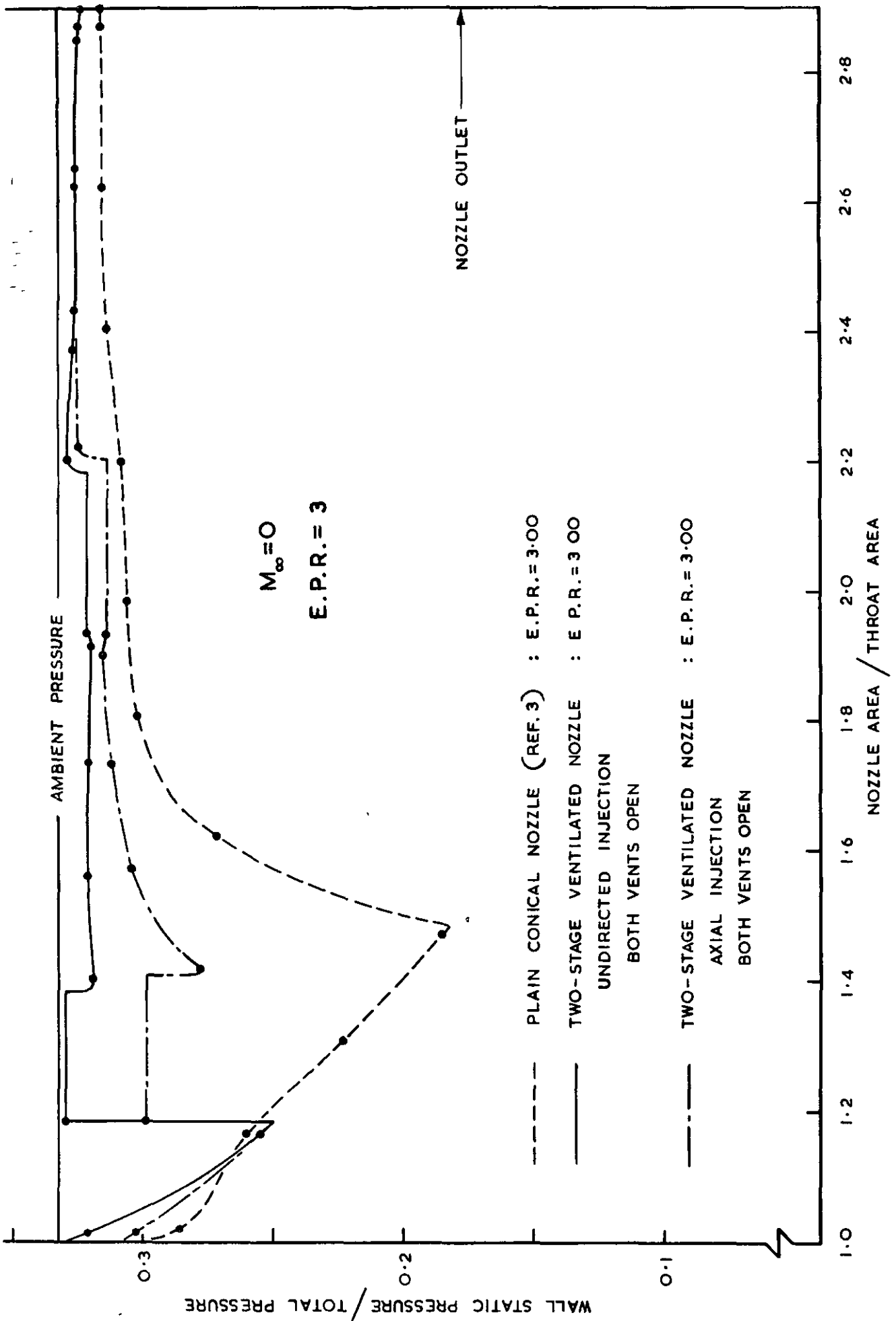


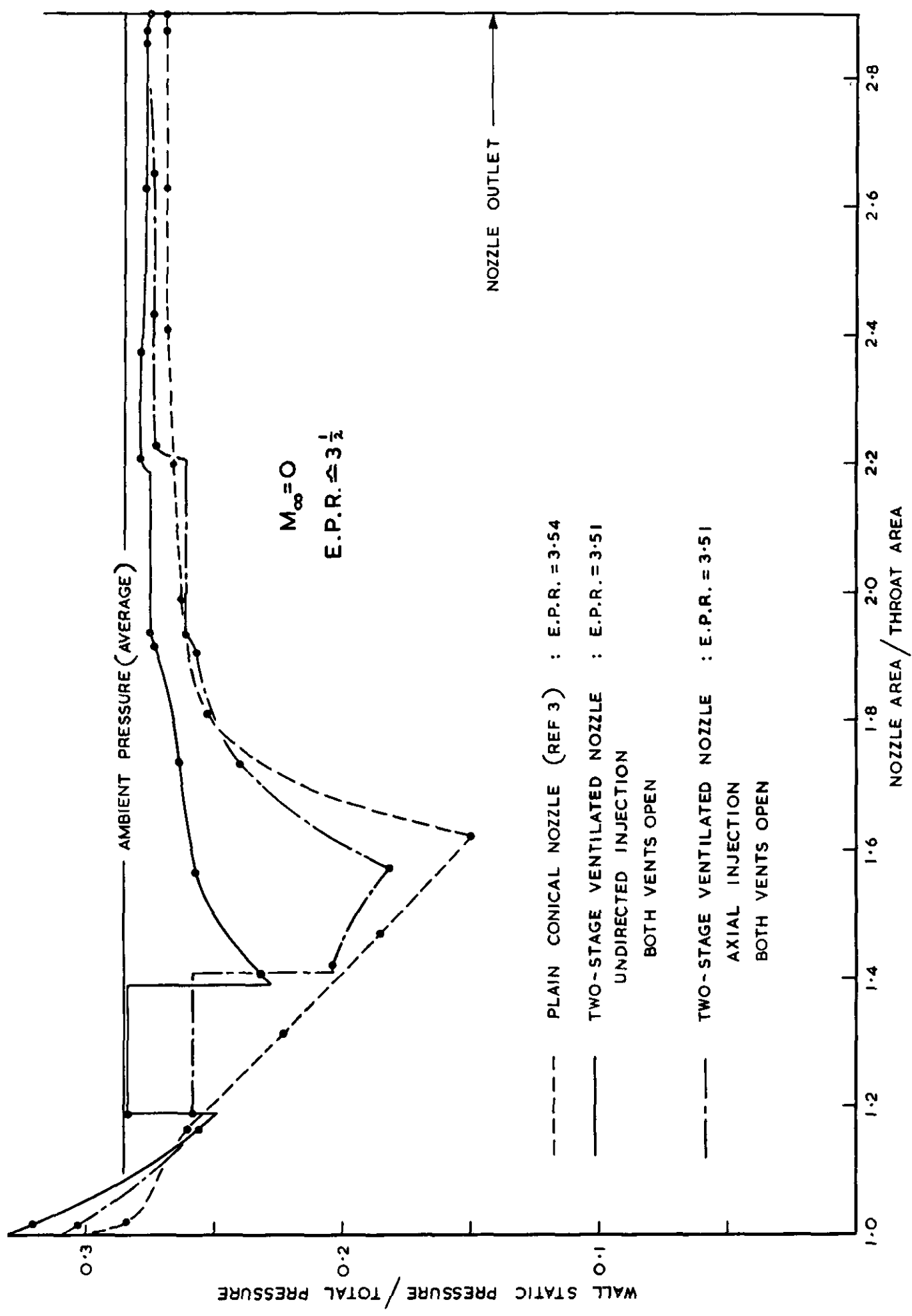
FIG.24a



TWO-STAGE NOZZLE PRESSURE DISTRIBUTION

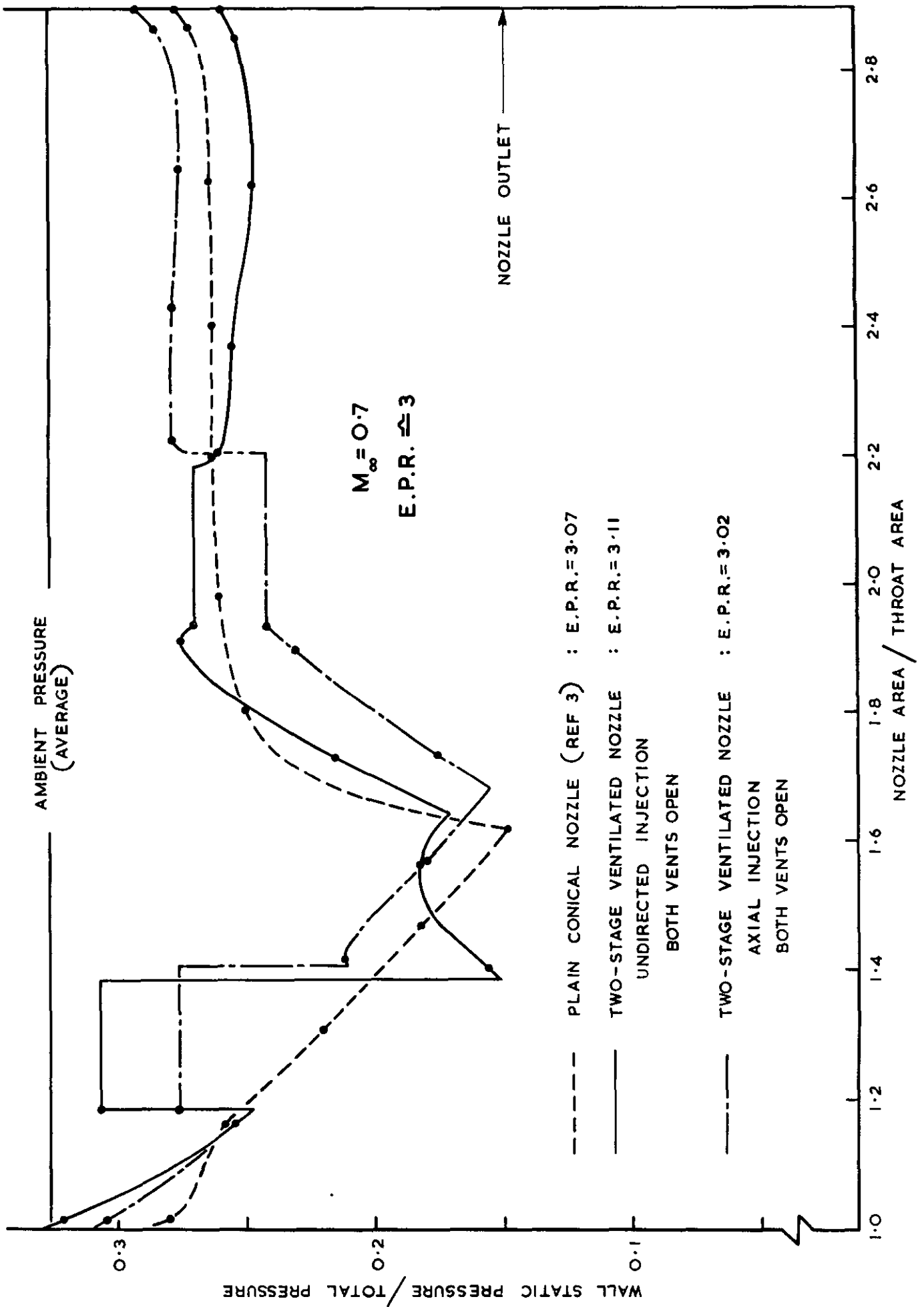


PRESSURE DISTRIBUTION IN VARIOUS NOZZLES



PRESSURE DISTRIBUTION IN VARIOUS NOZZLES

FIG.25c



PRESSURE DISTRIBUTION IN VARIOUS NOZZLES

PRESSURE DISTRIBUTION IN VARIOUS NOZZLES

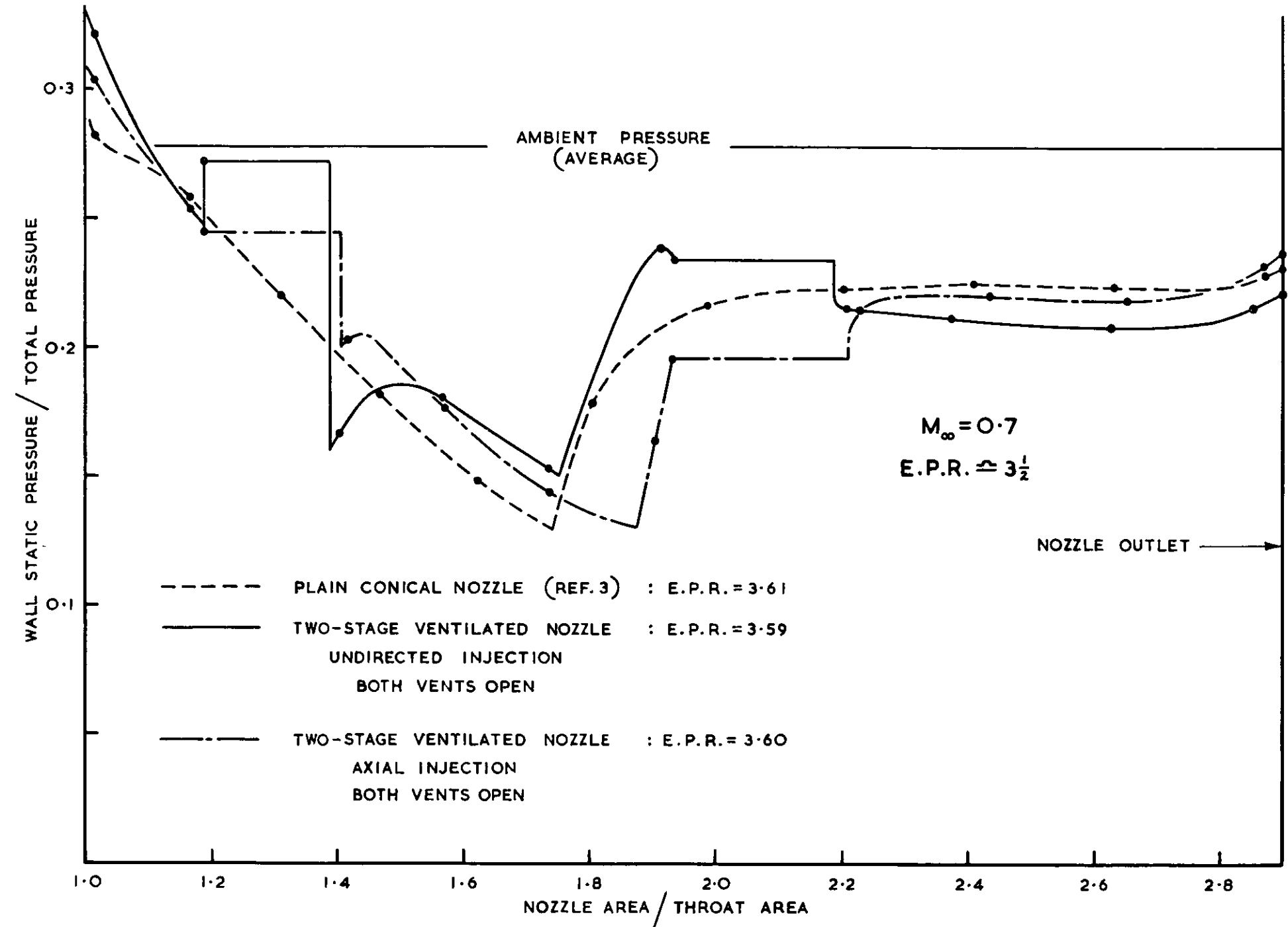


FIG. 254

PRESSURE DISTRIBUTION IN VARIOUS NOZZLES

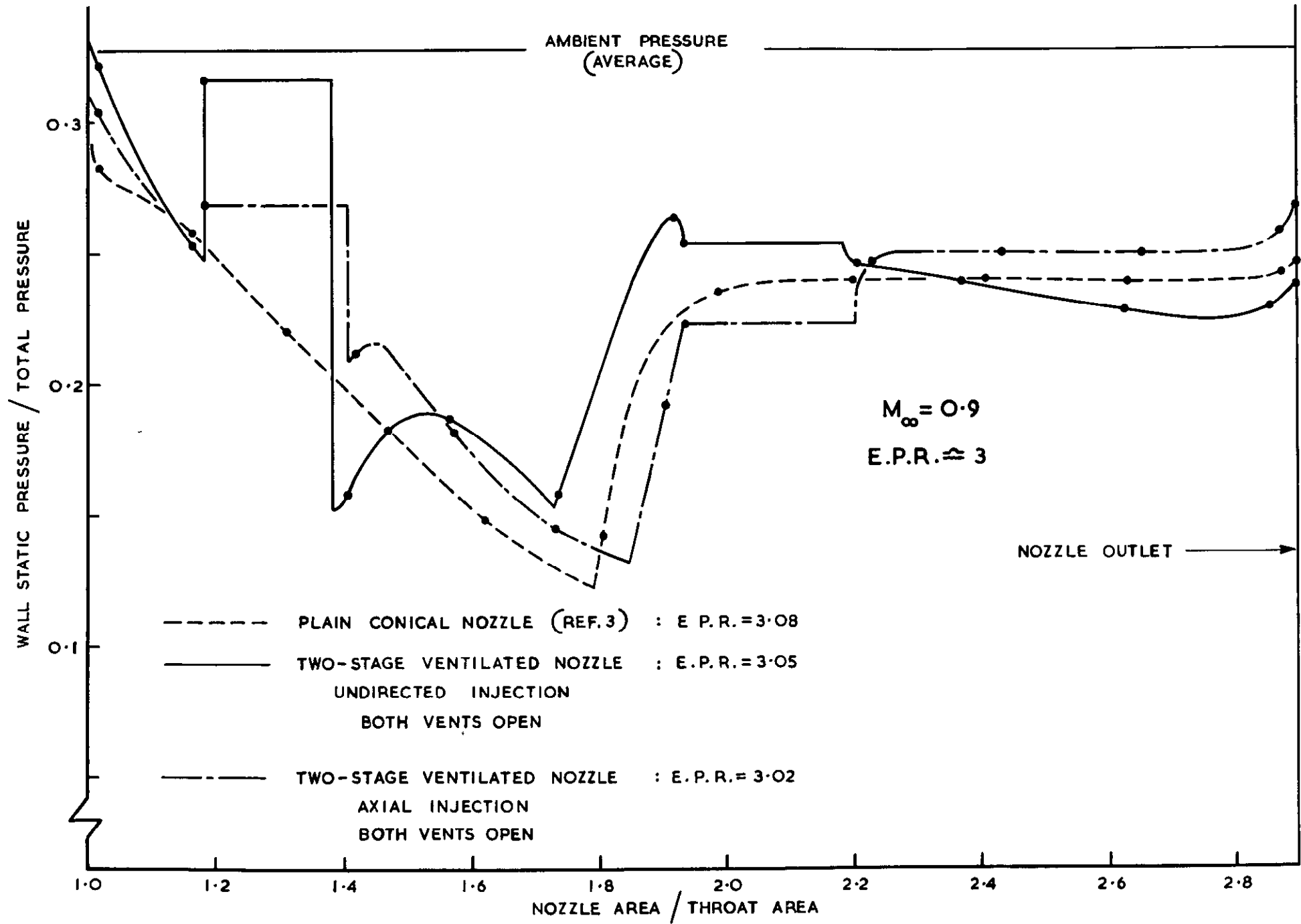
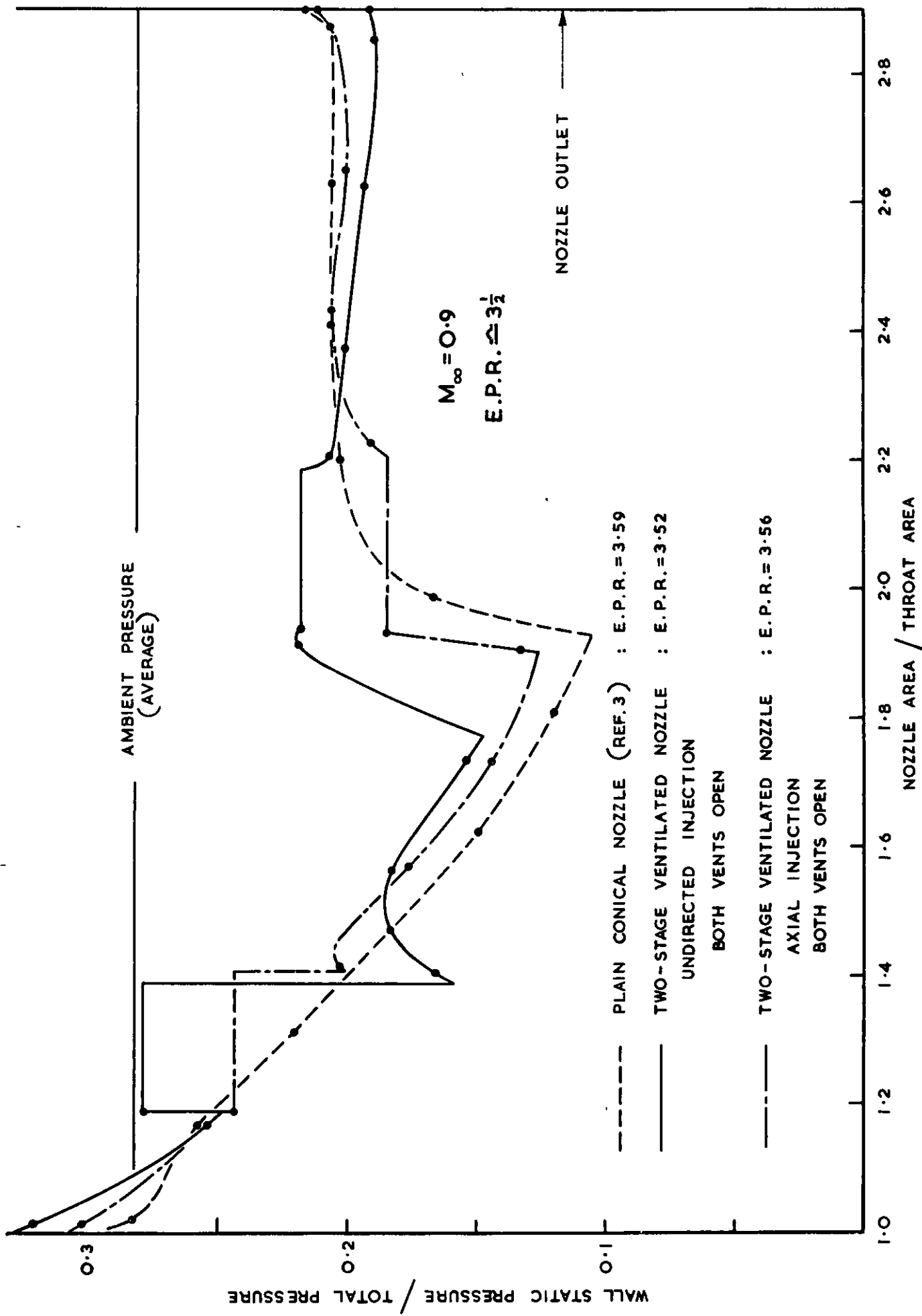


FIG. 25e



PRESSURE DISTRIBUTION IN VARIOUS NOZZLES



A.R.C. C.P.No.897
November, 1964

621-225.1:
533.691.18

Herbert, M. V., Overy, C., Pinker, R. A. and
Golesworthy, G. T.

THE EFFECT OF EXTERNAL FLOW ON AN INTERNAL-EXPANSION
PROPELLING NOZZLE INCORPORATING VENTILATION BY AMBIENT AIR

Previous attempts to improve the off-design performance of a convergent-divergent nozzle evolved the principle of "ventilation". This provides for the transmission of ambient pressure to the over-expanded divergent surfaces, by means of small quantities of secondary air induced from atmosphere. The technique has been developed to operate satisfactorily at low pressure ratio in quiescent air, using successive stages of secondary air admission. A penalty is paid, however, in that design-point performance is somewhat reduced. PTO.

A.R.C. C.P. No.897
November, 1964

621-225.1:
533.691.18

Herbert, M. V., Overy, C., Pinker, R. A. and
Golesworthy, G. T.

THE EFFECT OF EXTERNAL FLOW ON AN INTERNAL-EXPANSION
PROPELLING NOZZLE INCORPORATING VENTILATION BY AMBIENT AIR

Previous attempts to improve the off-design performance of a convergent-divergent nozzle evolved the principle of "ventilation". This provides for the transmission of ambient pressure to the over-expanded divergent surfaces, by means of small quantities of secondary air induced from atmosphere. The technique has been developed to operate satisfactorily at low pressure ratio in quiescent air, using successive stages of secondary air admission. A penalty is paid, however, in that design-point performance is somewhat reduced. PTO.

A.R.C. C.P. No.897
November, 1964

621-225.1:
533.691.18

Herbert, M. V. Overy, C., Pinker, R. A. and
Golesworthy, G. T.

THE EFFECT OF EXTERNAL FLOW ON AN INTERNAL-EXPANSION
PROPELLING NOZZLE INCORPORATING VENTILATION BY AMBIENT AIR

Previous attempts to improve the off-design performance of a convergent-divergent nozzle evolved the principle of "ventilation". This provides for the transmission of ambient pressure to the over-expanded divergent surfaces, by means of small quantities of secondary air induced from atmosphere. The technique has been developed to operate satisfactorily at low pressure ratio in quiescent air, using successive stages of secondary air admission. A penalty is paid, however, in that design-point performance is somewhat reduced. PTO.

In external flow, low nozzle base pressures are created, supplanting ambient pressure as the environment into which the nozzle exhausts. With a fairly high subsonic or transonic external stream, ventilation has been found incapable of raising the level of base pressure. Under these conditions, the technique offers no useful improvement in nozzle internal performance at low pressure ratio.

In external flow, low nozzle base pressures are created, supplanting ambient pressure as the environment into which the nozzle exhausts. With a fairly high subsonic or transonic external stream, ventilation has been found incapable of raising the level of base pressure. Under these conditions, the technique offers no useful improvement in nozzle internal performance at low pressure ratio.

In external flow, low nozzle base pressures are created, supplanting ambient pressure as the environment into which the nozzle exhausts. With a fairly high subsonic or transonic external stream, ventilation has been found incapable of raising the level of base pressure. Under these conditions, the technique offers no useful improvement in nozzle internal performance at low pressure ratio.

© *Crown copyright 1966*

Printed and published by

HER MAJESTY'S STATIONERY OFFICE

To be purchased from

49 High Holborn, London w c 1

423 Oxford Street, London w 1.

13A Castle Street, Edinburgh 2

109 St Mary Street, Cardiff

Brazennose Street, Manchester 2

50 Fairfax Street, Bristol 1

35 Smallbrook, Ringway, Birmingham 5

80 Chichester Street, Belfast 1

or through any bookseller

Printed in England